

POLITECNICO DI TORINO

**Corso di Laurea Magistrale
in Ingegneria Energetica e Nucleare**

Tesi di Laurea Magistrale

**INTEGRATION OF BIOMASS GASIFICATION
AND HIGH TEMPERATURE STEAM
ELECTROLYSIS FOR SYNTHETIC NATURAL GAS
(SNG) PRODUCTION**



Supervisors

**prof. Andrea Lanzini
ing. Emanuele Giglio
prof. Massimo Santarelli**

**Candidate
Gianluca Vitale**

March 2019

Contents

Abstract.....	9
1. Introduction.....	11
1.1. Research Objective	12
2. Technology review.....	17
2.1. Gasification	17
2.1.1. Types of gasifier	19
2.1.2. Syngas clean-up	24
2.2. Solid oxide electrolytic cell	28
2.2.1. Polarization curve	31
2.2.2. Use of steam as sweep gas	33
2.3. Methanation.....	35
2.4. Other.....	39
2.4.1. Water gas shift.....	39
2.4.2. Carbon capture and storage	40
3. Process modelling.....	45
3.1. General aspects	45
3.2. Drying section	48
3.3. Gasification section.....	50
3.3.1. Gasification performances.....	52
3.4. Methanation line	63
3.5. Solid oxide electrolytic cell unit.....	65
3.6. Rankine cycle	67
4. Process integration and efficiency.....	70
4.1. Process integration	70
4.1.1. First configuration.....	72
4.1.2. Second configuration.....	76
4.2. Thermal integration	80
4.2.1. First configuration.....	80
4.2.2. Second configuration.....	84
4.3. Energy efficiency.....	88

5. Conclusions	91
Bibliography	93

List of figures

Figure 1 - Total Primary Energy Supply (ktoe) by source per year [1]	11
Figure 2 - Simplified flowsheet of the first configuration	13
Figure 3 - Simplified flowsheet of the second configuration	13
Figure 4 - Tars distribution with temperature.....	19
Figure 5 - Schematic view of (a) downdraft (b) updraft and (c) crossdraft gasifiers [9]	20
Figure 6 - Schematic view of (a) bubbling and (b) circulating bed gasifier [9]	22
Figure 7 - Schematic view of an entrained flow gasifier	24
Figure 8 - Conceptual set-up of the SOEC technology for water electrolysis [7].....	28
Figure 9 - Thermodynamic of water electrolysis.....	30
Figure 10 - Polarization curve for an electrolytic cell.....	32
Figure 11 - Conceptual scheme of the SOEC utilized in this work	34
Figure 12 - Evolution of CO methanation with varying pressure and temperature	35
Figure 13 - Evolution of CO ₂ methanation with varying pressure and temperature	36
Figure 14 - Evolution of the contemporary CO and CO ₂ methanation with varying pressure and temperature	37
Figure 15 - Scheme of a post combustion system applied to a natural gas combined cycle power plant [13]	41
Figure 16 - Scheme of an oxy-combustion coal-fired power plant with CO ₂ capture [13]	42
Figure 17 - Scheme of an integrated gasification combined cycle with pre combustion capture [13]	42
Figure 18 - Simulation model of biomass drying.....	48
Figure 19 - Simulation model of the gasification section.....	50
Figure 20 - Effects of equivalence ratio on temperature of gasification	54
Figure 21 - Effects of equivalence ratio on syngas composition	55
Figure 22 - Influence of steam-to-biomass ratio on temperature of gasification	56
Figure 23 - Influence of steam-to-biomass ratio on syngas composition	57
Figure 24 - Influence of the type of biomass on temperature of gasification	59
Figure 25 - Influence of the type of biomass on syngas composition.....	60
Figure 26 - Effect of the temperature of the gasifying agent on the temperature of gasification.....	61
Figure 27 - Effect of the temperature of the gasifying agent on the composition of the syngas produced.....	62
Figure 28 - Simulation model of the methanation line	63
Figure 29 - Simulation model of the solid oxide electrolytic cell unit.....	65
Figure 30 - Simulation model of the Rankine cycle	67
Figure 31 - Detailed flowsheet of the first configuration of the plant.....	73

Figure 32 - Detailed flowsheet of the second configuration of the plant	77
Figure 33 - Preliminary integration of some fluids in the first configuration.....	81
Figure 34 - Composite curves resulting from the pinch analysis applied to the first configuration.....	83
Figure 35 - Composite curves resulting from the pinch analysis applied to the second configuration.....	86

List of Tables

Table 1 - Elements required for proximate, ultimate and sulphur analysis.....	46
Table 2 - Properties of the investigated biomasses	58
Table 3 - Gasification conditions for both configurations of the plant	70
Table 4 - Main streams of the first configuration of the plant.....	75
Table 5 - Main streams of the second configuration of the plant	79
Table 6 - List of streams involved in the thermal integration	82
Table 7 - Results of the pinch analysis applied to the first configuration	82
Table 8 - Results of the simplified network method applied to the first configuration	83
Table 9 - Heat balance for the second configuration	84
Table 10 - List of streams involved in the thermal integration	86
Table 11 - Results of the pinch analysis applied to the second configuration.....	86
Table 12 - Results of the simplified network method applied to the second configuration	87
Table 13 - Parameters for the calculation of the energy efficiency of the first layout..	88
Table 14 - Parameters for the calculation of the energy efficiency of the second layout	89
Table 15 - Comparison of energy efficiency with the different thermal integration method	89

Nomenclature

AC: Alternating Current

AEC: Alkaline Electrolytic Cell

ASR: Area Specific Resistance

ASU: Air Separation Unit

CCS: Carbon Capture and Sequestration

DC: Direct Current

DME: DiMethyl Ether

DTU: Denmark Technical University

ER: Equivalence Ratio

HHV: Higher Heating Value

LHV: Lower Heating Value

MEA: MonoEthanolAmine

NG: Natural Gas

OCV: Open Circuit Voltage

PEMEC: Proton Exchange Membrane Electrolytic Cell

PP: Pinch Point

PSA: Pressure Swing Adsorption

RES: Renewable Energy Sources

RR: Reactant Ratio

RU: Reactant Utilization

SNG: Synthetic Natural Gas

SOEC: Solid Oxide Electrolytic Cell

SOFC: Solid Oxide Fuel Cell

StB: Steam to Biomass

VSA: Vacuum Swing Adsorption

WGS: Water Gas Shift

YSZ: Yttrium Stabilized Zirconia

Abstract

Two different process configurations for the production of synthetic natural gas (SNG) starting from woody biomass are proposed and analyzed.

Both configurations are characterized by the integration of a two-stage gasifier, a solid oxide electrolysis cell (SOEC) system and a methane synthesis reactor. They differ in the size of the SOEC unit: in the first configuration electrolysis directly enhances the syngas produced in order to satisfy the stoichiometric requirement of the methanation reaction, while in the second one it provides to the gasifier the requested amount of gasifying agent (oxygen and steam). For this second configuration, an additional section composed by a water gas shift (WGS) reactor and a carbon capture and sequestration (CCS) unit is required to adjust the reacting gas composition and thus to ensure the proper stoichiometry for the methanation process. The two different configurations have been compared at the same gasification conditions.

The gasification unit has been studied to choose proper values of the gasification parameters, as equivalence ratio and steam-to-biomass ratio, and their impact on gasification outlet temperature and syngas composition.

The whole process has been analyzed from a thermodynamic standpoint using Aspen PlusTM.

After a thermal integration between the streams of the plant, energy efficiency has been calculated for both configurations: the first one (SOEC sized on hydrogen requirement) presents an efficiency of 73,1 %, while the second one (SOEC sized on oxygen requirement) shows an efficiency of 68,5 %.

1. Introduction

Biofuels are fuels generated directly or indirectly from biomass, which is one of the most important renewable energy source, due to its abundance and its homogeneous distribution all over the world.

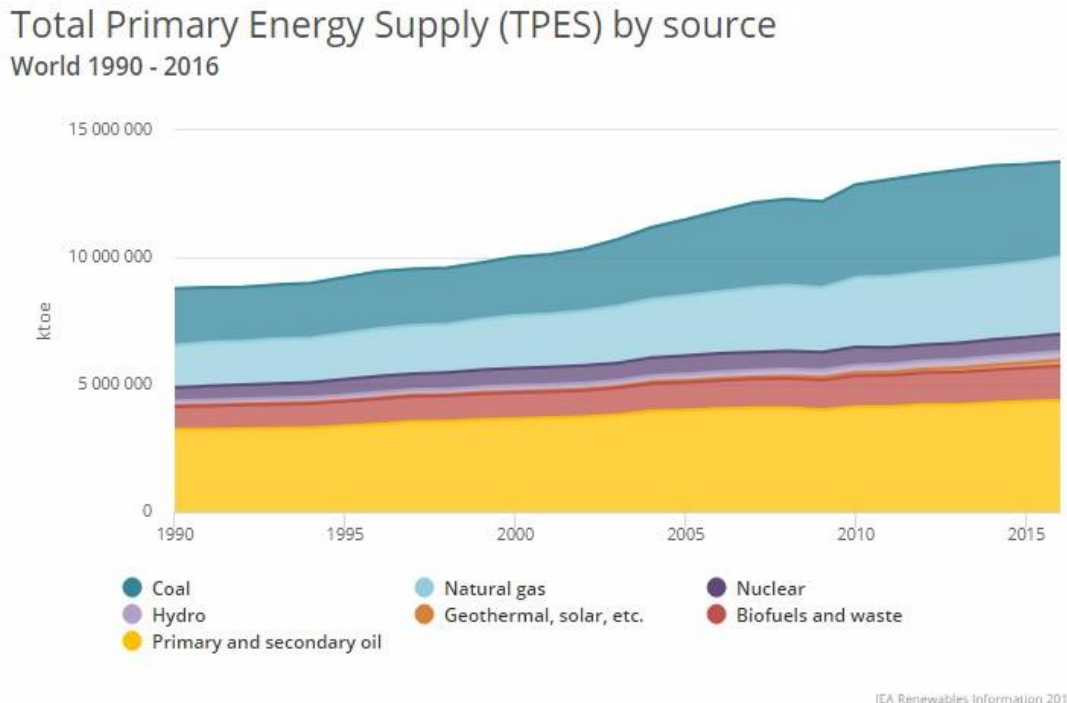


Figure 1 - Total Primary Energy Supply (ktoe) by source per year [1]

It can be seen in Fig. 1 that the percentage of energy supplied by biofuels, by the year 2016, represents around 10% of the total primary energy supply.

It is important to stress the fact that biomass does not add CO₂ to the atmosphere, since it absorbs CO₂ while growing, and then the CO₂ returns to the atmosphere when biomass is used as feedstock.

On the other hand, Natural Gas (NG) is a major primary fuel in global economy and, looking again Fig. 1, it is responsible, roughly, of the 20% of the total primary energy supply.

NG is used mostly for industrial and residential purposes, but recently its use is also diffusing in the transportations sector, in order to reduce the greenhouse gases emissions (according to the Kyoto protocol), for which this sector is responsible for 24% of the total fossil CO₂ emissions. [2]

In this context, processes that convert biomass into Synthetic Natural Gas (SNG) are of great interest.

1.1. Research Objective

The objective of this work is to model a plant in which biomass is used for the production of SNG, by means of the integration of a gasifier and an electrolytic cell.

Previous works, in literature, have already analyzed the integration of such systems to produce biofuels and chemicals: Pozzo et al. [3] have studied a biomass-to-dimethyl ether (DME) process, consisting of a biomass gasification unit integrated with a high-temperature co-electrolysis module; Clausen et al. [4] have modeled a methanol plant, consisting of a fluid bed gasifier, an alkaline electrolyzer and a steam reformer; Bernical et al. [5] have presented a model based on biomass gasification and high temperature steam electrolysis, followed by Fischer-Tropsch synthesis producing naphtha, gasoline, kerosene.

Finally Clausen again [6] has investigated a system for the thermochemical conversion of very wet biomasses (with a moisture content of 70 wt.%), integrating steam drying, solid oxide electrolytic cell (SOEC) and gasification for the production of SNG.

In this work, beech wood is considered as input biomass: it is first dried through hot air, and then gasified. The as produced syngas is then upgraded through a SOEC in order to satisfy the requirement of the subsequent methanation reactor. To run the water electrolysis, the SOEC needs a certain electrical power, which is taken from the grid.

Two different configurations have been considered: in the first one, the SOEC is dimensioned so to provide the syngas with the amount of hydrogen necessary to match the requirement of the methanation reactor; in the second configuration, the SOEC is dimensioned in order to supply the right quantity of gasifying agent to the gasifier. For this reason, to adjust the ratio before methanation reactor, it is used a Water Gas Shift (WGS) reactor and a Carbon Capture and Sequestration (CCS) section. Fig.2 and Fig.3 show simplified flowsheets of the described systems. These configurations have been compared at the same conditions of gasification.

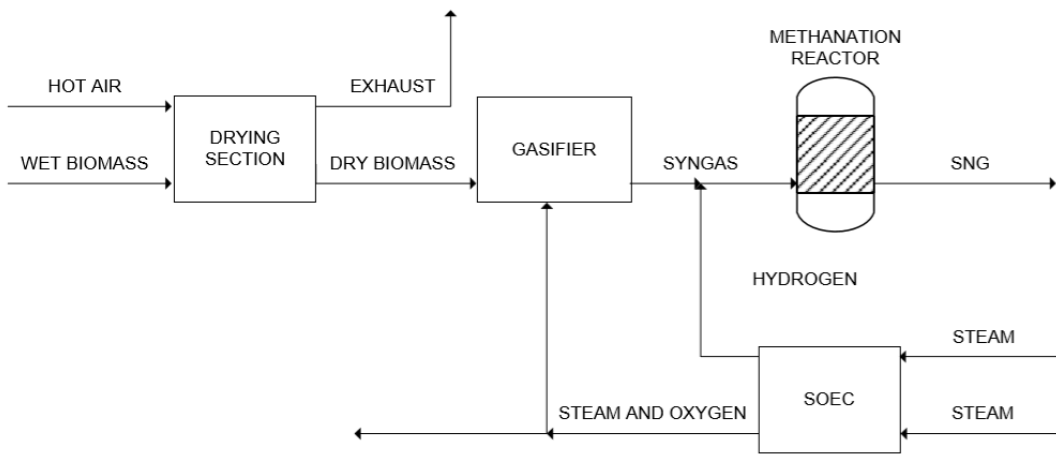


Figure 2 - Simplified flowsheet of the first configuration

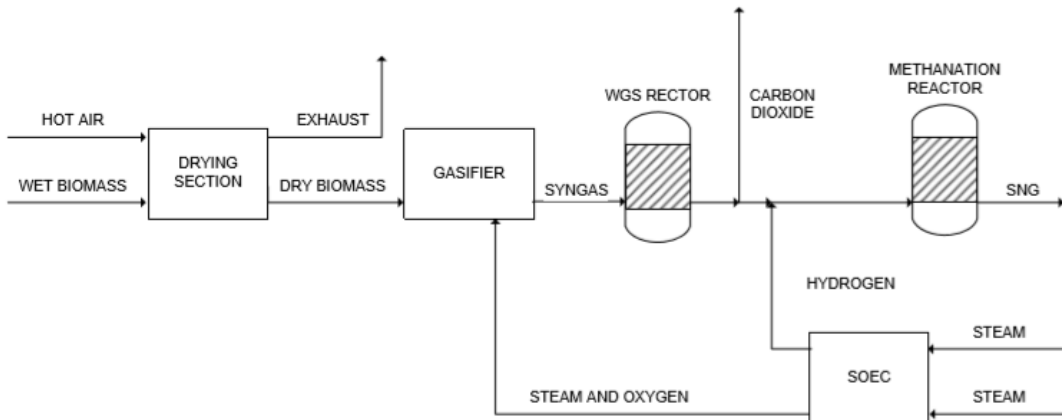


Figure 3 - Simplified flowsheet of the second configuration

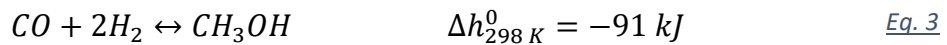
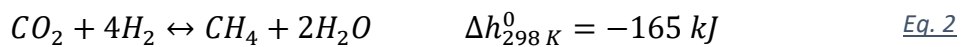
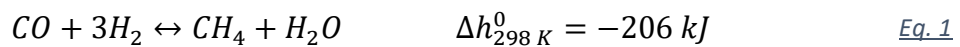
The modeling of these plants has been performed using Aspen Plus™ software: the results have been obtained with a zero-dimensional model. This represents a simplifying assumption which does not take into account thermal gradient along the SOEC stack as long as local kinetics. This fact could lead to differences of results between the models and the real systems.

Finally, a thermal integration is performed, in order to maximize overall plant efficiency, computed as first-principle efficiency.

Choice of the biofuel to produce

Integrating gasifier and electrolytic cell, as said before, is possible to produce many different types of biofuels but the choice fell on SNG because methanation reactions are highly exothermic with respect to the synthesis reactions of other biofuels.

Let's compare for example the methanation reactions (Eq.1,2) and the synthesis reactions of methanol (Eq.3,4):



It can be seen that methanation reactions release more than double the amount of heat per CO or CO₂ molecule with respect to the synthesis reactions of methanol. This means more heat available for the thermal integrations. [6]

Choice of the water electrolyzer

Actually, there are two mature and commercially diffused solutions regarding water electrolysis, both operating at low temperatures. The first one is the Alkaline Electrolytic Cell (AEC), which is based on a liquid electrolyte (aqueous solution with potassium hydroxide) operating in a temperature range of 60-80 °C. AEC systems are widely available, durable and exhibit relative low capital cost, but the low current density impacts negatively system size and hydrogen production costs. The second one is the Proton Exchange Membrane Electrolytic Cell (PEMFC), which uses a polymer electrolyte acid membrane as a medium of ion transfer and is characterized by an operating temperature between 50°C and 80°C. PEMFC has a higher current density and higher cell efficiency than AEC and allows the supply of highly compressed and pure hydrogen. Disadvantages include expensive catalyst (typically platinum), high system complexity due to high pressure operation and water purity requirements and shorter lifetime than AEC.

However, nonetheless it's the least developed electrolysis technology and it's not yet widely commercialized, the choice has fallen on the SOEC because it assures higher efficiencies associated with lower cost of the hydrogen produced. For this reason, it represents the type of electrolyzer on which the research is focusing most, trying to prevent the severe material degradation due to high operating temperatures (650-1000°C), enabling the commercialization of this technology. [7]

Choice of the type of gasifier

A two-stage downdraft gasifier operating at nearly atmospheric pressure is used to convert biomass into syngas. The main reasons of this choice are high cold gas efficiency (around 89-93 %, depending on the ash content) and very low tar content in the syngas produced. Indeed, the Viking gasifier concept, which is an example of two-stage gasifier developed by DTU, provides an abatement of tars 10000 times higher than conventional updraft gasifiers.

The gasifying agent is represented by the anode outlet, thus oxygen and steam, used as sweep gas in the SOEC.

2. Technology review

2.1. Gasification

Gasification is a chemical process that occurs in a deficient oxygen environment to convert carbonaceous materials into a gaseous product or synthesis gas, mainly composed by hydrogen H₂ and carbon monoxide CO, with lower amounts of carbon dioxide CO₂, water H₂O, methane CH₄, higher hydrocarbons and undesirable gases (like nitrogen N₂, sulphidic acid H₂S and chloridric acid HCl).

The gasification process is performed in presence of a gasifying agent that could be air, oxygen, steam or a mixture of these ones. It takes place at elevated temperatures between 500 and 1400 °C and at atmospheric or elevated pressure (until 70 bars).

Gasification utilizes various types of carbon based feedstocks, like coal, petroleum, petcoke, biomass and industrial waste.

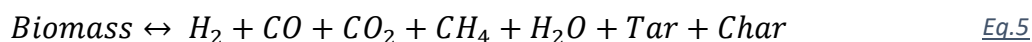
The principal reactions of gasification are endothermic and the necessary energy for their occurrence is granted by the partial oxidation of part of the biomass, thus ensuring an auto-thermal system.

Considering an auto-thermal system, gasification can be seen as a sequence of different steps. These steps are usually preceded by a drying stage, in order to reduce the moisture content of the inlet biomass.

The main steps of the gasification process are:

- Pyrolysis, which is an endothermic stage;
- Oxidation, which is an exothermic stage;
- Reduction, which is an endothermic stage;
- Tar decomposition, which is an endothermic stage.

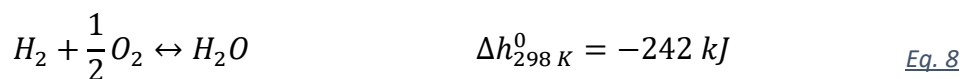
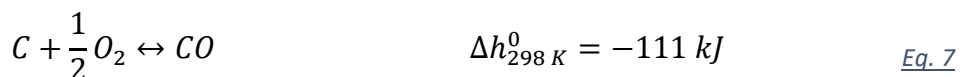
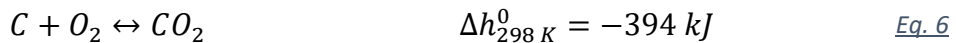
Pyrolysis or devolatilization consists in the thermochemical decomposition of the chemical bonds of the biomass particles, leading to the formation of molecules with a lower molecular weight. This step can be schematized with the following overall reaction:



Eq.6 shows that different fractions can be obtained by pyrolysis: a solid fraction, that includes the inert materials contained in biomasses in the form of ashes and a high carbon solid called “char”; a liquid fraction, commonly known as “tar”, constituted by complex organic substances condensable at relatively low temperatures; a gaseous fraction, which consists essentially of hydrogen H₂, carbon monoxide CO, carbon dioxide

CO_2 and light hydrocarbons, like methane CH_4 . The percentages of each fraction depend, essentially, on the type of gasifier and on the type of biomass used.

Oxidation of part of biomass is necessary to produce the thermal energy that will be used in the endothermic steps. It is carried out in lack of oxygen with respect to the stoichiometric value, in order to oxidize just a part of the biomass. It is possible to make the assumption that only carbon and hydrogen contained in the biomass participate to partial oxidation reactions. Under this hypothesis, the main reactions that take place are the following:



In the reduction step the products of the steps previously described react each other, leading to the formation of the final syngas. Main reactions occurring in this phase are:



Reactions described by Eq.10 and Eq.11, respectively Boudouard and reforming of the steam reaction, are endothermic, while reactions described by Eq.12 and Eq.13, respectively water gas shift and methanation reaction, are exothermic. The temperature at which the reduction step is carried out has a fundamental role in determining the composition of the syngas produced. Indeed, the endothermic reactions are favored at high temperatures, while the exothermic ones are favored at low temperatures.

For what concerns tars, they are defined as all the organic compounds with molecular weight greater than benzene. With respect to the other contaminants, tar is the most abundant per unit weight of biomass gasified and, for this reason, has been the focus of the majority of contaminant remediation studies.

Tars can be classified into primary, secondary and tertiary. Primary tars arise directly during the pyrolysis step and mainly depend on the type of biomass. Secondary tars can be formed during the oxidation step, as a consequence of the increase in temperature that may allow for the rearrangement of the primary tars. Finally, a further increase of temperature can lead to the decomposition and recombination of secondary tars and thus to the formation of tertiary or high temperature tars. Primary and tertiary tars don't coexist since tertiary tars appear only when primary tars are completely converted into secondary.

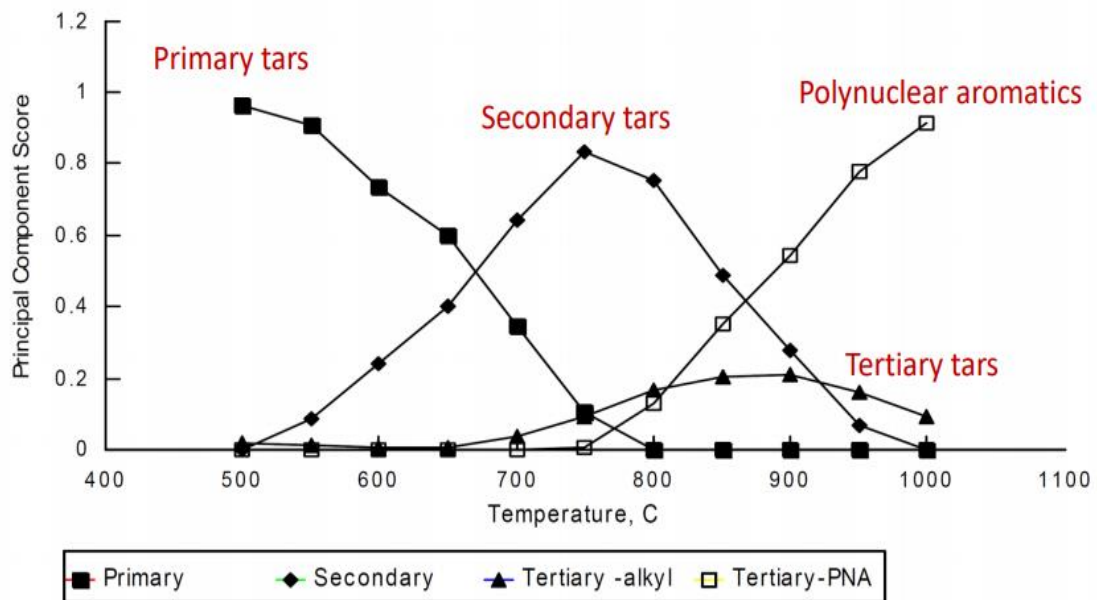


Figure 4 - Tars distribution with temperature

Tars removal or their conversion is the greatest challenge to overcome; actually different approaches are being followed, like bed thermal tar cracking or bed catalytic tar reforming. [8]

2.1.1. Types of gasifier

Different biomass gasifier types have been developed. Main criteria of differentiation are:

- Types of contact between the feed material and the gasifying agent, that could be counter-current, co-current or cross flow;
- Mode and rate of the heat transfer, i.e. the heat can be transferred from outside or directly in the reactor;

- Residence time of the feed material in the reaction zone, that can be in the order of hours or minutes.

The main typologies of gasifiers are:

- Fixed bed gasifiers;
- Fluidized bed gasifiers;
- Entrained flow gasifiers.

Fixed bed gasifiers

Fixed bed gasifiers are the simplest kind of gasifiers, consisting of a cylindrical vessel for fuel and gasifying agent, fuel feeding unit, ash collection unit and syngas exit. They are usually made of concrete or steel and generally work at moderate pressure conditions, low gas velocity, high carbon conversion and long residence time of the feed material. Fixed bed gasifiers are further distinguished in downdraft, updraft and crossdraft gasifiers.

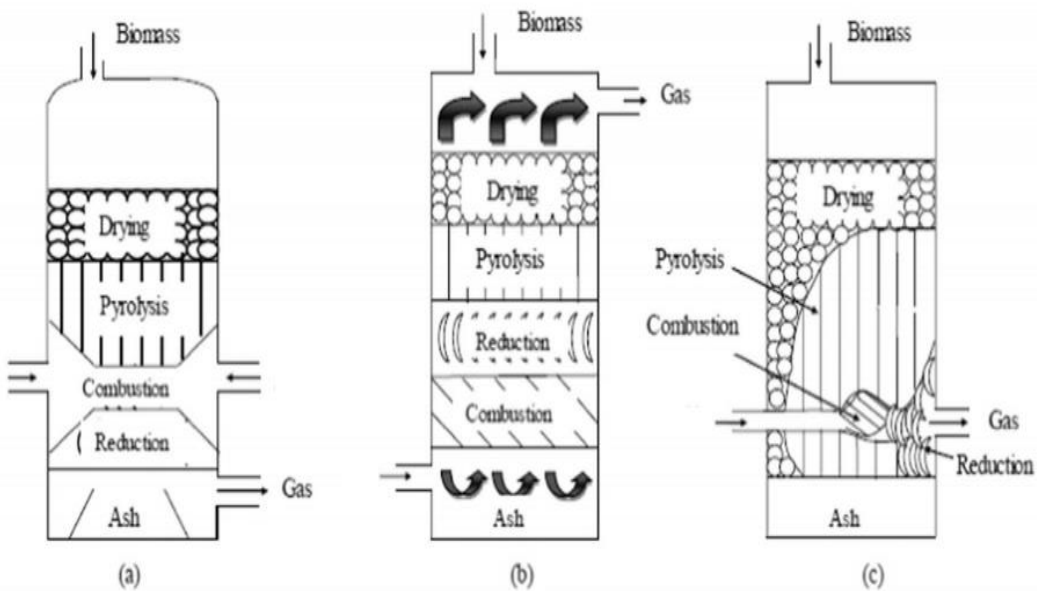


Figure 5 - Schematic view of (a) downdraft (b) updraft and (c) crossdraft gasifiers [9]

In downdraft gasifiers, the gasifying agent interacts with the solid biomass in the downward direction and, for this reason, they are called also co-current gasifiers. All the decomposition products from pyrolysis are forced to pass in the oxidation zone for thermal cracking and so it is possible to produce a high quality syngas with less tar content. Main advantages are high carbon conversion and low production of tar. Disadvantages are the requirement of biomass with a low moisture content, the

difficulty of starting and controlling the temperature and the limited possibility of scale-up (the dimensions are limited by problems of temperature control).

In the updraft gasifier, the gasifying agent enters from the bottom and moves towards the top, while the biomass is loaded from the top and moves downward. Hence, these gasifiers are also called counter-current gasifiers. A grate is present at the bottom of the gasifier, where the biomass is ignited. The hot gas moves upward transporting heat for the other stages of gasification and then leaves the gasifier at low temperature. Main advantages of updraft gasifiers are good thermal efficiency, small pressure drop, slight tendency to slag formation and the capability to handle biomass with high moisture content. Disadvantages are high tar content, low production of syngas, long start up time and poor reaction capability.

In crossdraft gasifiers, biomass enters from the top and the thermochemical reactions occur progressively as it descends in the reactor, while the gasifying agent enters at high velocity in the reactor from the sides, rather than from the top or the bottom. Main advantages are small start-up time, production of high temperature syngas and short design height. Disadvantages are the incapability of handling high tar content and very small fuel particles. However, crossdraft gasifiers are not so commonly used.

Fluidized bed gasifiers

Fluidized-bed gasifiers suspend feedstock particles in an oxygen-rich gas so the resulting bed within the gasifier acts as a fluid. These gasifiers are adequate for stationary processes, therefore are usually suitable for medium to large-scale installations. They usually produce a gas with high particulate content; therefore, a cyclone is usually a part of the installation. The gas temperature at the outlet is relatively high (800–900 °C). These gasifiers are meant to produce more tar than downdraft gasifiers but less than updraft gasifiers. The two most common configurations are bubbling fluidized bed and circulating fluidized bed.

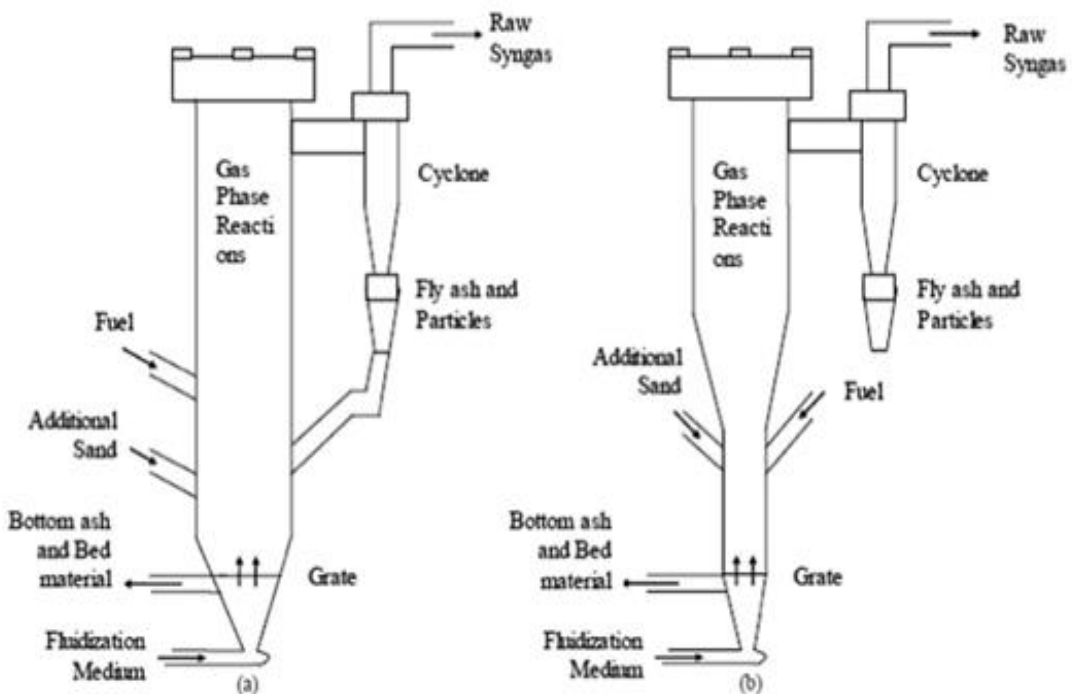


Figure 6 - Schematic view of (a) bubbling and (b) circulating bed gasifier [9]

Bubbling bed gasifiers are very simple in construction and operation. The gasification of biomass particles takes place under high pressure fluidized gasifying agent, allowing to pass through the reactor bed having inert bed materials such as sand, dolomite, etc. Generally, these gasifiers are designed to operate at a very low gasifying agent velocity (typically below 1 m/s). The solid particles while moving along the gas flow are separated from the gas in cyclone and get collected in the bottom of the fluidized bed reactor. Most of the part of conversion process takes place within the bubbling bed region and further extend lesser for tar conversion. They are capable of operating at the high average temperature of 850 °C and hence, more thermal decomposition of feedstock can be reported. However, the carbon conversion efficiency of bubbling bed gasifier is observed to be lower than those of the circulating fluidized bed gasifier due to stickiness behaviour of biomass particle which leads to the reduction of contact area between the particles.

In circulating bed gasifier, the solids, entrained with the high fluidizing gasifying agent velocity, are recycled back to the bed reactor to improve the carbon conversion efficiency which is low in the case of bubbling bed gasifier. These gasifiers are designed to operate at a higher gasifying agent velocity, ranging from 3 to 10 m/s. As compared to the bubbling fluidized bed reactor, the energy throughput per unit of reactor cross-sectional area has been reported higher. However, despite the improving carbon

conversion efficiency, these types of gasifier suffer from significant tar and dust related problems as well. But both are designed to operate under pressurized conditions for further increase in the yield of final product. Since the process of gasification is comprised of several complex physiochemical reactions which are very difficult to monitor externally and hence, has been the keen interest of researchers from the beginning of this area of research.

Entrained flow gasifiers

In entrained-flow gasifiers, the biomass fine particles (0.1–1 mm particles) and the gasifying agent are injected in co-current. Entrained-flow gasifiers operate at high temperature (1300–1500°C) and pressure (25–30 bar), and are characterized by an extremely turbulent flow which causes rapid feedstock conversion and allows high throughput. The gasification reactions occur at a very high rate (typical residence time is of the order of a few seconds), with high carbon conversion efficiencies (98–99.5%). Given the high operating temperatures, gasifiers of this type melt ash into vitreous inert slag. The biomass fine particles can be delivered in either a dry or slurry form. A pneumatic feeding is usually used to inject pressurized powder solid fuels into the gasifier, while slurries are atomized and subsequently fed as pulverized solid fuel. The slurry feed is a simpler operation, but it introduces water into the reactor which requires heat to evaporate. The result of this additional water supply is a syngas with a higher H₂/CO ratio, but with lower gasifier thermal efficiency. The feeding system needs to be properly designed along with the other process parameters. The high temperatures tend to shorten the life of the system components, including the vessel refractory.

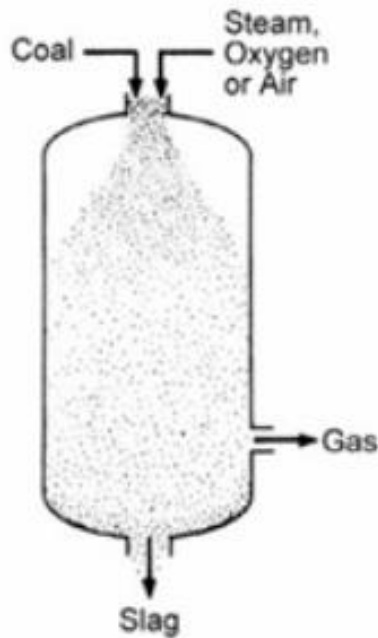


Figure 7 - Schematic view of an entrained flow gasifier

2.1.2. Syngas clean-up

In the context of gasification, contaminants are condensable organic compounds known as tar, nitrogenous compounds like ammonia (NH_3) and hydrogen cyanide (HCN), sulfur containing inorganic compounds like hydrogen sulfide (H_2S), carbonyl sulfide (COS) and carbon disulfide(CS_2), hydrogen halides and halogens such as hydrogen chloride (HCl) and chlorine (Cl), and trace metals like sodium(Na) and potassium (K). These contaminants emanate from volatile organic and inorganic constituents in biomass and are consequently present at widely varying concentrations in syngas.

The presence of these contaminants in syngas causes several technical and operational issues like equipment corrosion or fouling, catalyst deactivation and environmental pollution.

Thus, raw syngas clean-up is an essential step prior to syngas utilization in downstream applications. Main techniques of syngas clean-up are grouped in two categories: cold gas clean-up and hot gas clean-up.

Cold gas clean-up

Cold gas clean-up represents commonly the conventional approach in syngas clean-up because of its proven reliability and high contaminant removal efficiency. This approach

is carried out at low temperature (usually at or below room temperature) and so, as gasification is carried out at high temperatures, the main disadvantage is the efficiency penalty due to syngas cooling and the additional cost incurred to treat or dispose of contaminant streams.

Cold gas clean-up utilizes wet or dry processes: wet cold gas clean-up processes employ spray and wash towers, impingement and wet electrostatic precipitators or cyclones. These units remove contaminants by absorption and adsorption, filtration or a combination of those ones. In contrast, dry cold gas clean-up processes employ mechanical, physical and electrostatic separation including cyclones, adsorbing bed and other filters, dry electrostatic precipitators, etc. Among the two types of cold gas clean-up approaches, wet cold gas clean-up processes are more commonly used because they easily allow for multiple-contaminants removal.

Cold gas tar clean-up is carried out by wet scrubbing with a liquid absorbent. The selection of the solvent is important in order to maximize the removal efficiency. Water is commonly used for scrubbing tars from syngas because it is cheaper. However recent researches have been focused on oil-based absorbents which afford a higher removal efficiency, but increase cost and complexity of the process.

Cold gas clean-up of nitrogen containing contaminants is conventionally carried out through wet scrubbing. Because of the high solubility of NH₃ and HCN in water, water based scrubbing is regarded as the conventional approach for cold gas removal of nitrogen containing contaminants. Using this approach, deleterious nitrogen species removal is often carried out simultaneously with tars. The benefits of conventional wet scrubbing of syngas through water is the significant reduction of NH₃ concentrations with removal efficiency greater than 99%.

Cold gas clean-up of sulphur contaminants in syngas can be realized with wet or dry cleaning processes. For wet gas clean-up, there are two modes of sulphur removal in solvent: chemical reaction or physical absorption. In alternative, dry cold gas removal of sulphur contaminants can be carried out on porous sorbents like activated carbon or metal impregnated activated carbon.

Finally, HCl and other hydrogen halides are commonly removed by wet scrubbing usually through a caustic solution (e.g. caustic water) or, alternatively, simply water. However, despite caustic water is a potential scrubbing solvent, water remains the most commonly used solvent.

Hot gas clean-up

Warm and hot gas clean-up techniques focus on contaminant removal from syngas at high temperature ($> 300^{\circ}\text{C}$). The advantage of hot gas clean-up consists in avoiding the loss in efficiency, which is a downside of cold gas clean-up. Additionally, it reduces the waste streams because of converting some contaminants into environmentally benign or even useful products. Over the years, group of catalysts have been tested in hot gas clean-up.

Tar compounds can be removed by thermal cracking, hydrocracking, steam or dry reforming. Thermal cracking is the conversion of tar to C and H₂ at elevated temperatures ($> 1100^{\circ}\text{C}$). Hydrocracking represents the tar decomposition in presence of hydrogen, producing methane. Moreover, tar can be converted to carbon monoxide and hydrogen through steam reforming or through dry reforming (using CO₂). Due to the high activation energy and its endothermic nature, steam reforming of tars occurs appreciably only above 900°C in the absence of a catalyst. When a suitable catalyst is employed, temperatures ranging between 650 and 900°C are sufficient for high conversion. However, tar steam reforming often suffers from catalyst deactivation through coke, although this can be minimized considerably by careful control of the steam to carbon ratio. Dolomite, olivine, limonite, calcium/magnesium carbonates as well as nickel based catalysts have been widely used in tar removal in bench-scale as well as pilot-scale setup.

Nitrogen containing contaminants are not easy to decompose under typical gasification temperature without the use of catalysts. The most effective active metals are Ni or Ni promoted with Ce or La, Co or Co-Zn mixed oxide, Ru and Fe while Al₂O₃ and activated carbon are among the most common and effective supports. In addition, limonite is also very effective in NH₃ decomposition. While the experimental conditions vary widely depending on the studies, NH₃ decomposition in the context of hot gas cleanup is typically investigated at temperatures ranging from 450 to 750C.

Unlike tars and ammonia, sulphur removal is achieved with the help of a sorbent, commonly a metal oxide, which chemically reacts with sulphur contaminants to produce a metal sulphide. This process is referred to, interchangeably as desulfurization, from the point of view of sulphur removal from syngas or sulphidation, from the point of view of metal oxide conversion to its corresponding metal sulphide. The most common catalysts employed in desulfurization are metal oxides with ZnO and CuO often regarded as the reference. But also calcium based sorbents are great of interest in gasification due to their relative lower cost.

Finally, the research on halide clean-up is not as exhaustive as that of tar, NH₃ and hydrogen sulphide, especially for biomass derived syngas. Hydrogen halides are removed from syngas via dehydrohalogenation. Thermodynamic simulations have

indicated that alkaline and alkali earth metals are promising halide sorbents for clean-up temperatures greater than 500°C. [10]

2.2. Solid oxide electrolytic cell

Solid oxide electrolytic cell (SOEC) is the least developed electrolysis technology. As electrolyte material, it uses solid ion-conducting ceramics (usually zirconia stabilized with yttrium YSZ), thus enabling operation at higher temperatures (700-900°C). For the fuel electrode (which is cathode in case of electrolysis), the most common used material is a porous cermet composed of YSZ and metallic nickel. For the oxygen electrode, instead, the material is usually the lanthanum strontium manganite LSM-YSZ composite.

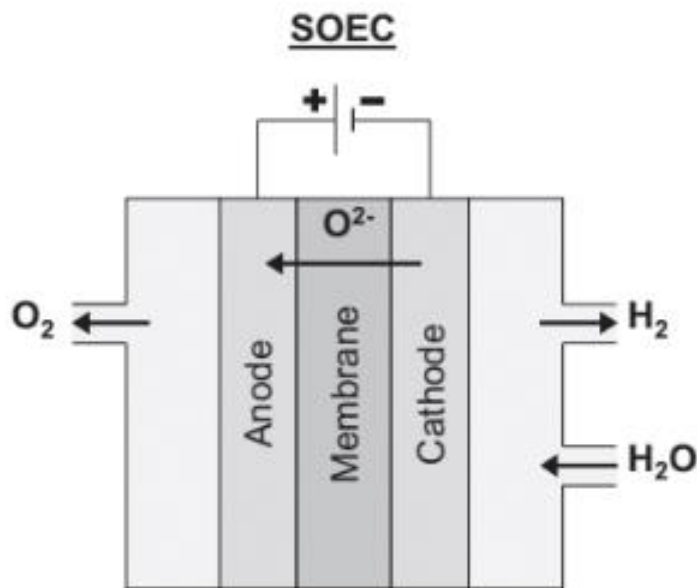


Figure 8 - Conceptual set-up of the SOEC technology for water electrolysis [7]

The reactions that take place in a SOEC are the inverse of those that take place in a solid oxide fuel cell (SOFC): water is the reactant and it is fed to cathode, where the following reaction takes place:



At the anode side, the reaction that takes place is:



Thus, the overall reaction becomes:



In order to avoid re-oxidation of the fuel electrode, a fraction of the cathode exhausts can be recirculated and, for this reason, the inlet stream to the cathode will contain some fraction of hydrogen. The Reactant Ratio (RR) takes into account this fact: it points out the reactant fraction of the inlet molar flow.

Furthermore, not all the reactant will effectively react in the stack; this is taken into account with the Reactant Utilization (RU), which indicates the percentage.

So, the fraction of inlet molar flow that effectively undertakes electrochemical reactions \dot{n}_R is related to the total inlet molar flow \dot{n}_{IN} through the following equation:

$$\dot{n}_R = \dot{n}_{IN} \cdot RU \cdot RR \quad \text{Eq.16}$$

High temperature electrolysis shows a great potential as the electrolysis of water is increasingly endothermic with increasing temperature, but the required electric power reduces at higher temperatures since the Joule heat of an electrolytic cell is used in this process.

The minimum electric energy supply needed by water electrolysis is equal to the variation of the Gibbs free energy, defined like:

$$\Delta G = \Delta H - T\Delta S \quad \text{Eq.17}$$

where:

ΔH represents the enthalpy variation;

T represents the temperature;

ΔS is the entropy variation.

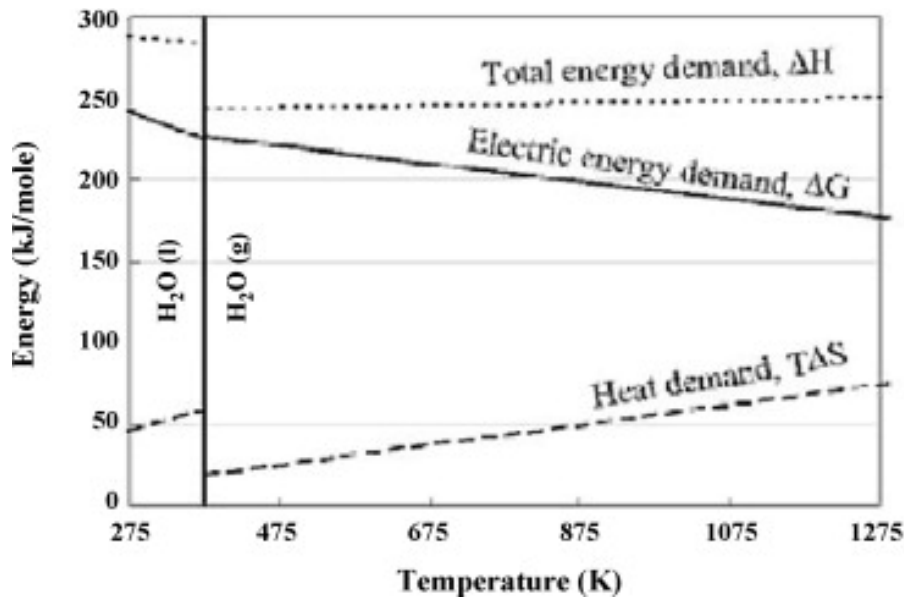


Figure 9 - Thermodynamic of water electrolysis

Fig.9 describes the thermodynamic of water electrolysis: it is possible to observe how ΔG decreases, even though total energy demand is increasing, since heat energy demand increases with increasing temperature at a fixed pressure. Operating at higher temperatures can therefore decrease the cost of the produced hydrogen, especially if the increase in heat energy demand can be satisfied by an external heat source.

So, since the thermal energy required for the electrolysis reaction can be replaced with the Joule heat generated in the cell as a consequence of the passage of electrical current through the cell, the electrical energy demand decreases and also the H₂ production price.

For this devices that operate in reverse conditions, the thermoneutral voltage can be defined:

$$V_{tn} = \frac{\Delta H}{n \cdot F} \quad \text{Eq.18}$$

where:

ΔH represents the total energy demand needed by the electrolysis reaction;

n represents the number of electrons involved in the reaction that, in the case of water electrolysis, is equal to 2;

F is the Faraday constant.

It represents that particular value of the voltage at which the generated Joule heat in the cell and the heat consumption due to electrolysis are equal.

Thus, for operating voltages lower than the thermoneutral one, the net heat flux is negative, while for operating voltages higher than the thermoneutral one, the net heat flux is positive.

2.2.1. Polarization curve

The relationship between voltage and current density is a fundamental characteristics of the cell efficiency and is generally calculated from Open Circuit Voltage (OCV).

OCV represents the difference of potential between the two terminals of the cell, when it is disconnected from any circuit. It can be estimated by using the Nernst equation:

$$OCV = \frac{\Delta G}{n \cdot F} \quad \text{Eq.19}$$

where:

ΔG is the Gibbs free energy variation;

n represents the number of electrons involved in the reaction that, in the case of water electrolysis, is equal to 2;

F is the Faraday constant.

The operating voltage deviates from the OCV because of some overvoltages caused by internal losses due to irreversible processes; main are:

- activation overvoltage η_{act} on both electrodes, that is due to two phenomena: the chemical equilibrium state of ions at the electrode-electrolyte interface and the overcoming of the electric field due to transfer of charged particles across the interface by ions. Activation overvoltage can be mitigated increasing temperature, active surface area or activity of the catalyst used.
- ohmic overvoltage η_{ohm} , caused by the resistance to conduction of ions in the electrolyte, conduction of electrons in the electrode and contact resistance. Most commonly, only ionic resistance of the electrolyte is considered, because other resistances are orders of magnitude lower and then negligible.
- diffusion overvoltage η_{diff} , very relevant at high current densities and mainly due to the transport phenomena (in particular mass transport)

All of the overvoltages previously described, grow with the current density, but we can distinguish different zones in which one of the mechanism previously described prevails over others.

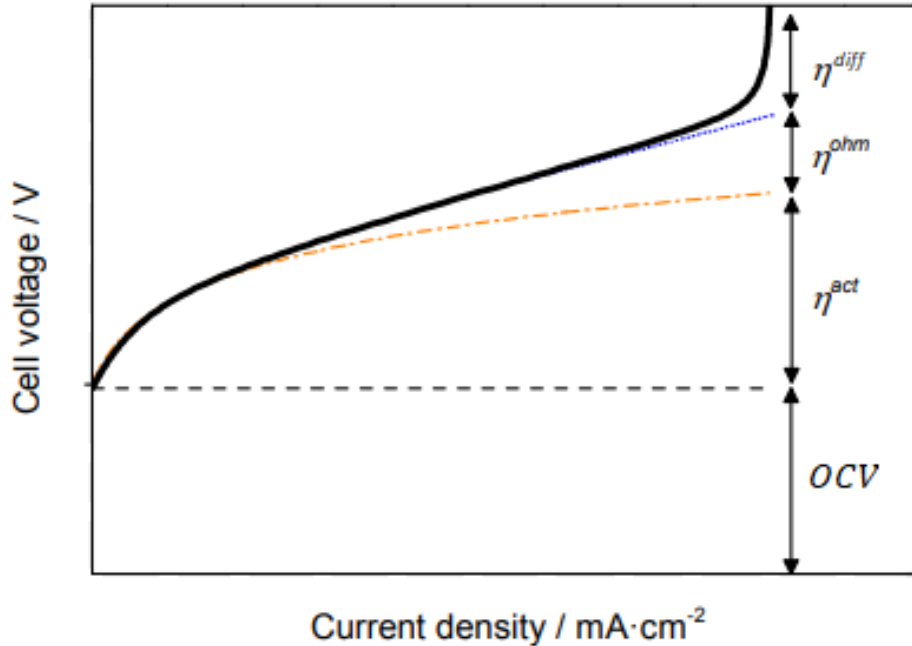


Figure 10 - Polarization curve for an electrolytic cell

Therefore, as it is possible to view from Fig.10, cell potential can be expressed like:

$$V_c = OCV + \eta_{act} + \eta_{ohm} + \eta_{diff} \quad \text{Eq.20}$$

A simplest model can be obtained assuming a linear relationship between voltage and current density (i.e. linearization of the polarization curve). This hypothesis is well justified for a SOEC since high temperatures enhance the kinetic of electrochemical reactions (increasing thus the rate of reaction and decreasing then the activation overvoltage) and improve the diffusion of reactants in electrodes (so decreasing the diffusion overvoltage). The slope of this first order curve is the Area Specific Resistance (ASR), defined as:

$$ASR = \frac{V_c - OCV}{j} \quad \text{Eq.21}$$

where:

V_c is the cell potential [V];

j is the current density [A/m^2].

In this way, it is possible to derive the following expression for the operating voltage as a function of the current density

$$V_c = OCV + j \cdot ASR \quad Eq.22$$

ASR is influenced by materials used for the electrolyte and the electrodes, geometrical features both macroscopic and microscopic and certainly operational parameters like temperature, pressure and inlet gas composition. [11]

Finally, the electrical power needed by the cell can be calculated as:

$$P_{el} = V_c \cdot j \cdot S \quad Eq.23$$

where:

V_c is the cell potential [V];

j is the current density [A/m^2];

S is the active surface of the cell [m^2].

2.2.2. Use of steam as sweep gas

The oxygen electrode (i.e. the anode) presents the higher contribution to ohmic losses during the operations and the higher degradation due to delamination of the electrode/electrolyte interface.

Moreover, high oxygen concentrations in the electrode get worse the electrolysis reaction and increase polarization losses. For this reason, generally, air is used as sweep gas to flow out oxygen from the anode and reduce oxygen concentration, because of its low cost and easy availability.

In this work, however, it has been used steam as sweep gas because it is already available in the system for the production of hydrogen in the SOEC and because it has been chosen to use a mixture of oxygen and steam as gasifying agent for the gasifier.

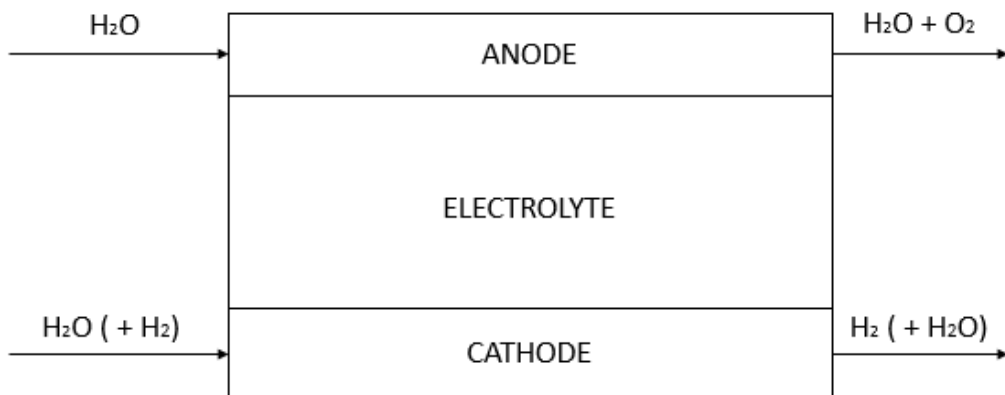


Figure 11 - Conceptual scheme of the SOEC utilized in this work

As a drawback, additional heat is necessary for the production of the steam that will be used as sweep gas.

Using steam as sweep gas shows another aspect particularly interesting: SOEC is not seen only as a hydrogen production device but, at the same time, as a pure oxygen generator. Indeed, pure oxygen has an important market value, even if it is not a fuel and no energy can be recovered from that molecule.

Actually, in order to obtain pure oxygen, air is treated in air separation plants, in which are used cryogenic distillation processes, based on several condensing reactors that separate liquid nitrogen from gaseous oxygen, or non-cryogenic processes, like pressure swing adsorption (PSA), vacuum swing adsorption (VSA), polymeric membranes or ion transport membranes.

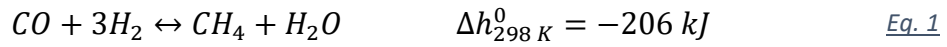
Making use of steam as sweep gas allows to produce a mixture of oxygen and steam at the oxygen electrode exit, from which oxygen can be easily separated just condensing water.

Regarding corrosion issue, both the presence of steam and hydrogen can cause material degradation but the doping of cathode composition or the use of special stainless steel can prevent the formation of contaminants.

In literature, Barelli et al. [12] have already demonstrated the feasibility of substituting air with steam on the oxygen electrode side without any decrease in performance, in terms of diffusion losses or material oxidation, and achieving the advantage of production of pure oxygen without any separation cost

2.3. Methanation

Methanation is a physical-chemical process to generate methane from a mixture of various gases out of gasification, source of carbon monoxide and dioxide. CO and CO₂ are hydrogenated according to the methanation reactions:



Both the reactions are strongly exothermic and are thermodynamically favored at low temperature and high pressure. However, the performance becomes poor at low temperatures below 200°C and too high pressure because of limitations in the reaction kinetics.

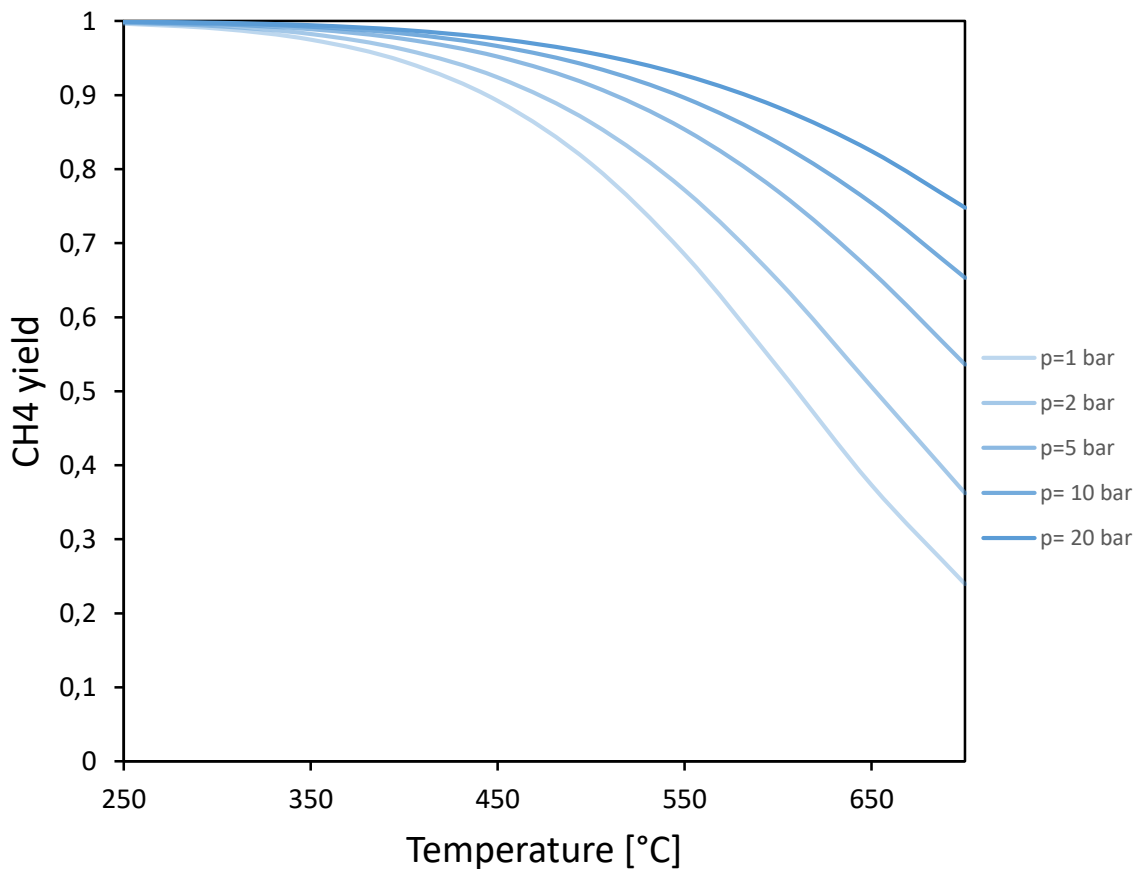


Figure 12 - Evolution of CO methanation with varying pressure and temperature

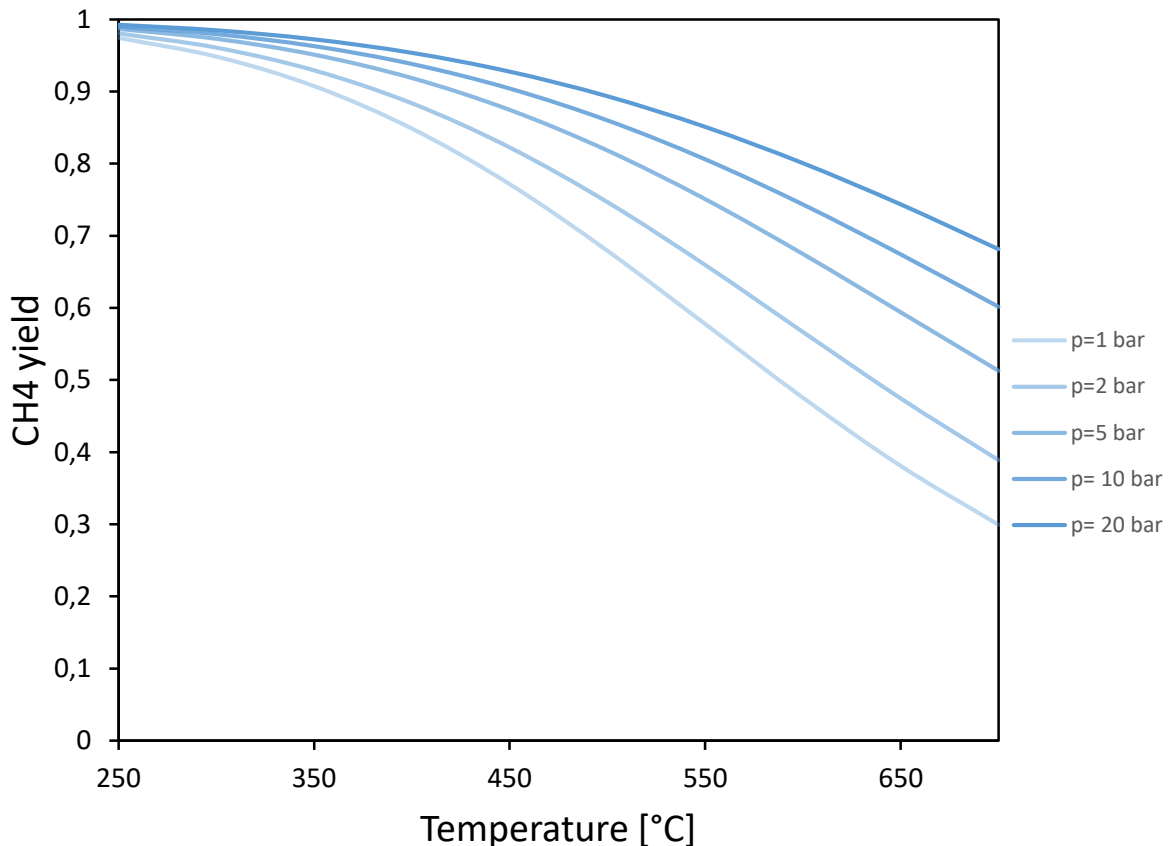


Figure 13 - Evolution of CO₂ methanation with varying pressure and temperature

In order to obtain a product with as high methane content as possible, it is important that the feed gas at the inlet of the methanation section have a composition with the correct ratio between the reactants, i.e. CO, H₂ and CO₂. The predominant methanation reaction is normally the methanation from CO, and from Eq.1 it can be seen that the stoichiometric ratio between H₂ and CO is 3. However, in order to take into account the content of CO₂ in the feed gas for methanation, the feed gas module has been developed:

$$FEED = \frac{y_{H_2} - y_{CO_2}}{y_{CO} + y_{CO_2}} = 3 \quad Eq.24$$

where y_i represents the molar fraction of the reactant i.

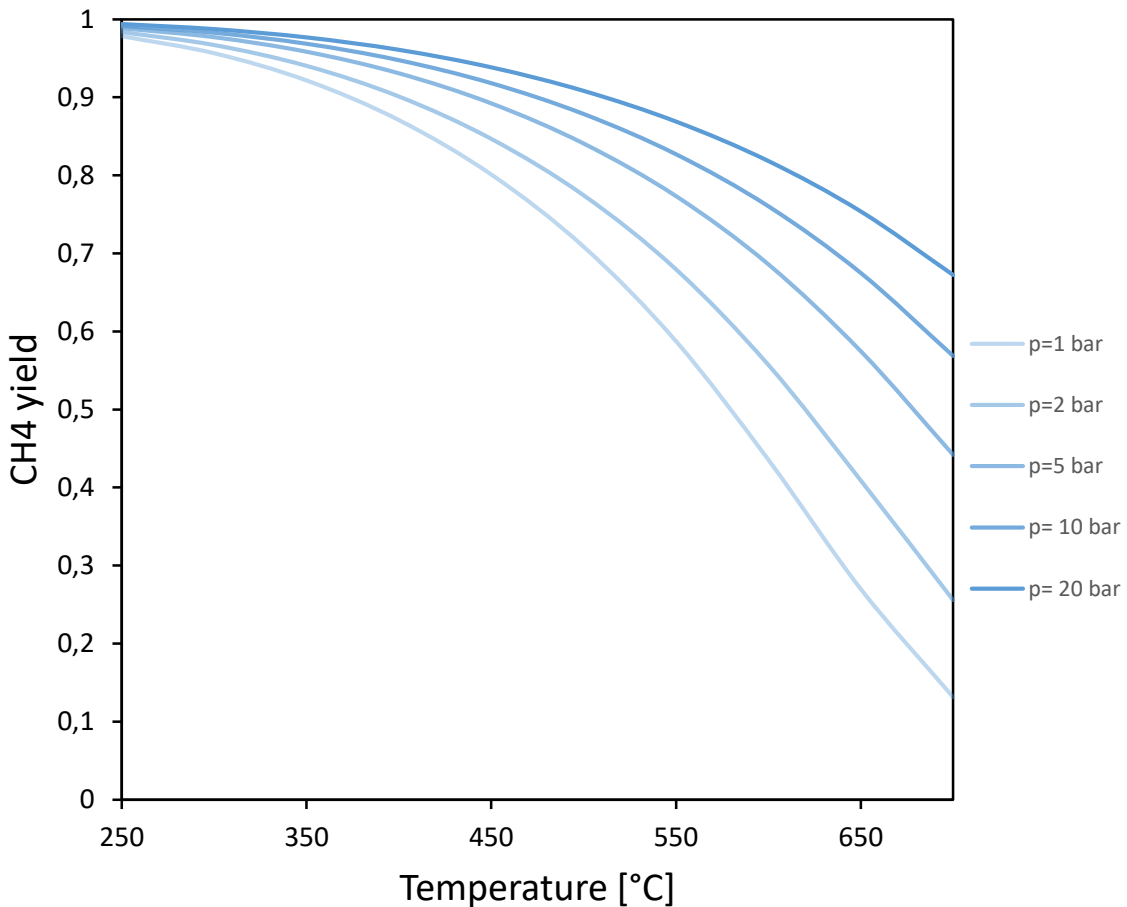


Figure 14 - Evolution of the contemporary CO and CO₂ methanation with varying pressure and temperature

Although methanation process is thermodynamically favored, the complete hydrogenation of the carbon oxide to methane consists of an eight-electron process characterized by significant kinetic limitations. It is, therefore, required the presence of a catalyst in order to achieve acceptable rates and high selectivity. A large variety of metals have been used as catalysts for the methanation reaction: the most common, and to some extent the most effective, appear to be nickel-based and ruthenium-based catalysts, because of their high activity and low price.

Almost all the commercially available catalysts used for this processes are very susceptible to sulfur poisoning, so efforts must be taken to remove all hydrogen sulphide before the catalytic reaction starts.

Moreover, large amounts of heat must be removed from the system to prevent high temperatures and deactivation of the catalyst by sintering as well as the deposition of carbon. In particular, the most critical aspect is represented by the catalyst temperature within the first reactor. The methanation reaction is strongly exothermal: even though the reactor is cooled, an initial temperature increase will take place in the first part of

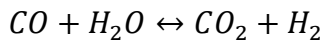
fixed bed, when the reactant concentration is still high. To eliminate this problem, temperatures should be maintained below 550°C, which is considered a threshold value to preserve the catalyst stability and to avoid unexpected degradation or loss of activity.

To control the maximum temperature, the ratio between the tube containing the fixed bed and the catalyst particle can be set, in order to avoid channeling phenomena within the catalytic bed. A decrease of the pipe diameter implies lower volume heat generation from the exothermal reaction. The number of tubes also affects the temperature profile along the reactor: a higher number of tubes implies a decrease of flow per tube. Therefore, the maximum achieved temperature will increase for two reasons. First, lower space velocity for the gas mixture in a single tube means higher conversion and thus higher heat production. Second, lower superficial velocity of the gas leads to worse heat exchange between the gas in the pipe and the surrounding coolant. On the other hand, a lower number of tubes implies higher velocity in the tube, causing an increase of the pressure drop that could become unacceptable.

2.4. Other Balance of Plant devices

2.4.1. Water gas shift

Water gas shift (WGS) reaction is an important industrial process in which water in the form of steam is mixed with carbon monoxide to obtain hydrogen and carbon dioxide, according to the reaction:



Eg. 11

WGS reaction is a reversible and moderately exothermic reaction ($\Delta h_{298\text{ K}}^0 = -41\text{ kJ}$) which proceeds with no variation in volume. Due to its moderate exothermicity, the reaction is thermodynamically unfavorable at elevated temperatures. Nevertheless, the kinetics of the catalytic reaction are more favorable at high temperatures. In order to overcome the thermodynamic limitation while maintaining high reaction rates, WGS is normally conducted in multiple adiabatic stages with intermediate acid gas removal, desulphurization and intercooling, if high purity hydrogen is needed. So high temperature shift occurs in the first stage, with a temperature range of 350°C to 600°C, while low temperature shift occurs in the second stage, in which temperatures ranges from 150°C to 300°C. However, if high purity hydrogen is not required a single stage reactor could be sufficient.

Reaction pressure does not have any effect on the equilibrium, since the number of moles of material does not change during the course of the reaction.

Different catalysts are employed in the two stages: usually, iron-based are used in the high temperature shift, while copper-based are employed in the low temperature shift. The iron-based catalysts are an example of some of the earliest heterogeneous catalysts used industrially. They can tolerate small quantities of sulphur and are quite robust overall. Copper-based catalysts represent a more recent development which has gained wide industrial acceptance. These catalysts have good activity at low temperatures and are therefore attractive. However, copper-based catalysts are completely sulphur intolerant, being irreversibly poisoned by even small quantities of sulphur compounds. Another material used as water gas shift catalyst is the sulphided cobalt oxide-molybdenum oxide on alumina, which is completely insensitive to sulphur and possess good activity at both high and low temperatures.

2.4.2. Carbon capture and storage

One method to reduce CO₂ emissions to the atmosphere includes carbon capture and sequestration (CCS), a process which consists in capturing waste CO₂, transporting it to a storage site where it is injected down wells and then permanently trapped in porous geological formations deep below the surface. The three steps comprising CCS are CO₂ capture, transport, and storage.

The first step of CCS is the capture which has the task to separate CO₂ from other gaseous substances. Technologically, this is considered to be the most difficult part of the entire mechanism. Actually, there are three main methods to separate the CO₂:

- Post combustion capture;
- Oxy-fuel capture;
- Pre combustion capture.

The post-combustion separation method involves separation of CO₂ from the flue gas after the power generation step. Main advantages of post combustion capture are the possibility of retrofitting all the existing power plants without any or with only minor modifications and the control of the energy demand of the plant by adjusting the CO₂ capture level or by bypassing the CO₂ capture step at the times of the peak loads. Due to the low concentration of carbon dioxide in flue gas, its partial pressure will be very low. Thus, chemical absorption is likely to be needed, but also temperature and pressure swing adsorption can be used. However, a large volume of pressure steam is required for the regeneration of the chemical solvent. A number of chemical solvents can be used for CO₂ capture through chemical absorption, such as amines, ammonia and potassium carbonate. Monoethanolamine (MEA) is by far the most popular solvent for chemical absorption based CO₂ capture. Reasons for all the inefficiencies of post-combustion capture include the low concentrations of CO₂ in flue gas, large volumes of flue gas to be treated, the requirement of compressing CO₂ from the atmospheric pressure to the storage pressure and the relative high temperature of the flue gas, which needs to be cooled before the CO₂ capture. Moreover, flue gas contains contaminants such as sulphur dioxide that are problematic to remove and negatively impact the performances of many technologies.

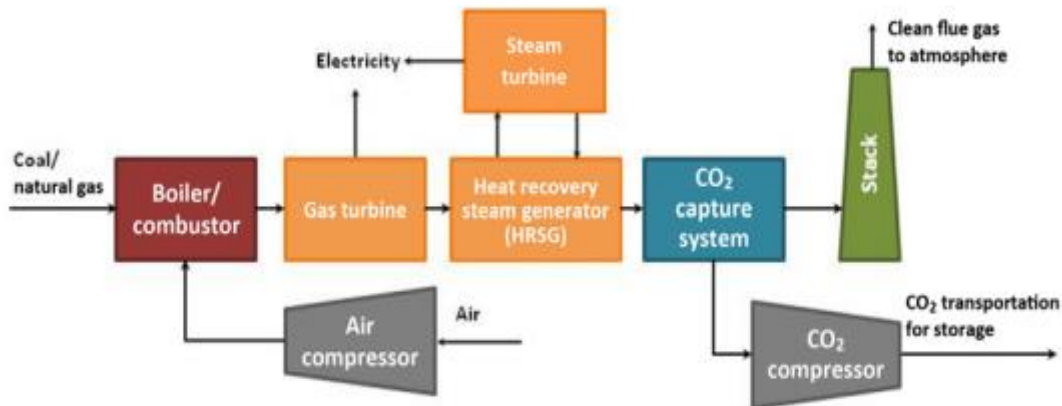


Figure 15 - Scheme of a post combustion system applied to a natural gas combined cycle power plant [13]

Oxy-fuel capture is a kind of post combustion capture, with the difference that the fuel, in the power generation step, is burnt with pure oxygen instead of air, so that the flue gas contains mainly CO₂ and water. Therefore, the CO₂ separation can be done simply by condensation of the water. The major advantage of oxy fuel combustion is that the cost of post combustion capture is much lower. However, the air separation unit (ASU), necessary to generate pure oxygen used for combustion, can be costly for a large scale power plant. Another challenge is that temperatures for oxy-fuel combustion are much higher than those for air combustion; therefore, a large amount of inert flue gas must be recycled to the boiler to maintain operating temperatures at levels similar to in air-combustion. Also, there is limited experience for this technology, since there is a lack of full scale demonstration power plants. Improvements are needed in the air separation by use of cryogenics and the development of alternative cost-effective oxygen production technologies. This technology can be applied to both new and existing plants. Oxy-combustion technology is still at an early stage of development, but some pilot plants are being built and there are advanced-stage plans for building commercial scale power plants.

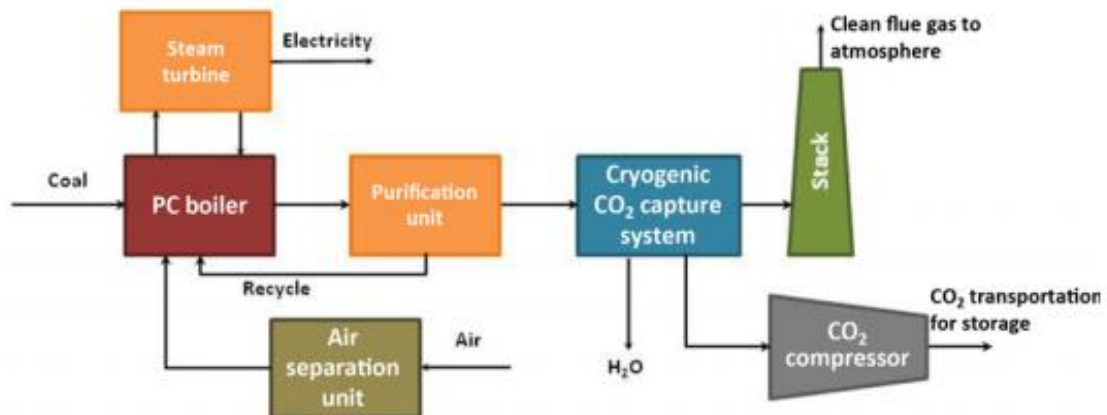


Figure 16 - Scheme of an oxy-combustion coal-fired power plant with CO₂ capture [13]

Pre combustion separation involves the capture of CO₂ from the syngas produced by the gasification of the fuel and processed in a water gas shift reactor, leaving just hydrogen for the power generation. The sulfur compounds are removed from fuel gas prior to the CO₂ capture. As compared to the post combustion capture, pre combustion capture is much easier and cheaper, but fuel conversion steps are costly. Physical absorption can be effective since the CO₂ concentration and pressure are higher. However, the gas stream needs to be cooled before physical absorption can be performed. Fuel gas after the capture needs to be heated back up before being sent to the combustion chamber. Temperature and pressure swing adsorption and membranes can also be employed for the CO₂ separation from hydrogen in pre-combustion capture.

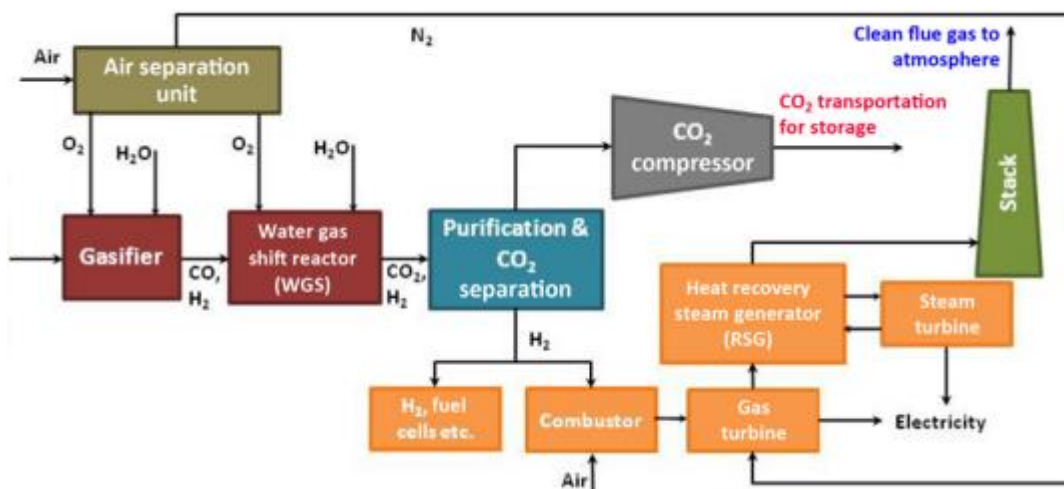


Figure 17 - Scheme of an integrated gasification combined cycle with pre combustion capture [13]

After CO₂ has been captured by any of the aforesaid methods, it needs to be transported to the storage site. This can be done in several ways, such as pipelines, boats, railways or trucks. However, pipelines transportation is considered to be most viable. The pipelines used must be of good quality as any compromise with it may lead to CO₂ leak. Of course, carbon dioxide is not combustible like natural gas, which is rather inflammable. So, CO₂ transportation is more of an economic rather than a technological barrier.

After the captured CO₂ has been transported to a potential storage site, it needs to be stored. The CO₂ may be stored in geological formations or oceans. The choice of the storage site depends upon the CO₂ storage potential and cost-effectiveness. CO₂ storage in oceans was initially conceived as a possible option, but due to very high environmental risks, it is no longer considered one.

3. Process modelling

3.1. General aspects

The commercial software Aspen PlusTM has been used to model the plants. It represents a process modelling tool for conceptual design, optimization and performance monitoring of chemical processes. Aspen PlusTM is provided of a large database of pure component and phase equilibrium data for conventional chemicals, electrolytes, solids and polymers and with reliable thermodynamic data, realistic operating conditions and rigorous equipment models allows to simulate actual plant behaviour, making use of engineering relationships such as mass and energy balances, phase and chemical equilibrium and reaction kinetics.

The hypothesis of chemical equilibrium has been applied to all chemical reactors, so no kinetic approaches has been considered.

Firstly, the stream class MIXCINC has been selected. Stream classes are used to define the structure of simulation streams; the selected one includes:

- Conventional streams (MIXED), i.e. vapour/gas and liquid streams and solid salts in solution chemistry;
- Conventional inert solids (CI), i.e. solids that are inert to phase equilibrium and salt precipitation/solubility, but take part to chemical equilibrium (using the Gibbs reactor);
- Nonconventional solids (NC), i.e. heterogeneous substances inert to phase, salt and chemical equilibrium that cannot be represented with a molecular structure.

No particle size distribution has been considered for the feed biomass.

To calculate the nonconventional solid properties, it is necessary to specify the “NC Props”. Because nonconventional components are heterogeneous solids that do not participate in chemical or phase equilibrium, the only physical properties that are calculated for nonconventional components are enthalpy and density. The HCOALGEN and the DCOALIGT models have been used to calculate them.

In particular, the model HCOALGEN uses the proximate analysis, ultimate analysis and sulphur analysis to calculate the enthalpy of the nonconventional solid considered.

Description	Elements
Proximate analysis, weight %	Moisture Fixed carbon Volatile matter Ash
Ultimate analysis, weight %	Ash Carbon Hydrogen Nitrogen Chlorine Sulphur Oxygen
Sulphur analysis, weight %	Pyritic Sulphate Organic

Table 1 - Elements required for proximate, ultimate and sulphur analysis

All the values of proximate, ultimate and sulphur analysis are defined as weight percentage on a dry basis, with the exception, of course, of moisture in proximate analysis.

The values need to meet the following consistency requirements: the sum of the values of the sulphur analysis must be equal to the value for sulphur specified in the ultimate analysis, the value for ash specified in the ultimate analysis must be equal to that one specified in the proximate analysis, the sum of the ultimate analysis values must be equal to 100 and the sum of the values of fixed carbon, volatile matter and ash must be equal to 100.

Subsequently, the components have been specified: BIOMASS and ASH as nonconventional solids, C as conventional inert solid and H₂O, N₂, O₂, NO₂, NO, S, SO₂, SO₃, H₂, Cl₂, HCl, CO, CO₂ and CH₄ as conventional streams.

For the nonconventional solid BIOMASS, it is necessary to specify the heat of combustion on a dry basis.

Finally, the thermodynamic method used to calculate properties of the conventional streams has been selected: the IDEAL property method (ideal gases, Raoult's law and Henry's law) has been selected for the drying and gasification section, while the PENG-ROB (Peng Robinson equation of state) property method has been selected for the other sections.

3.2. Drying section

The simulation model of the drying section is shown in Fig.18. A wet biomass stream and a hot air stream are fed to the drier, while a stream of dried biomass and a steam of moist air exit. It uses two-unit operation blocks to simulate a single piece of equipment and, for this reason, the extra stream that connect the two simulation blocks has not a real physical meaning.

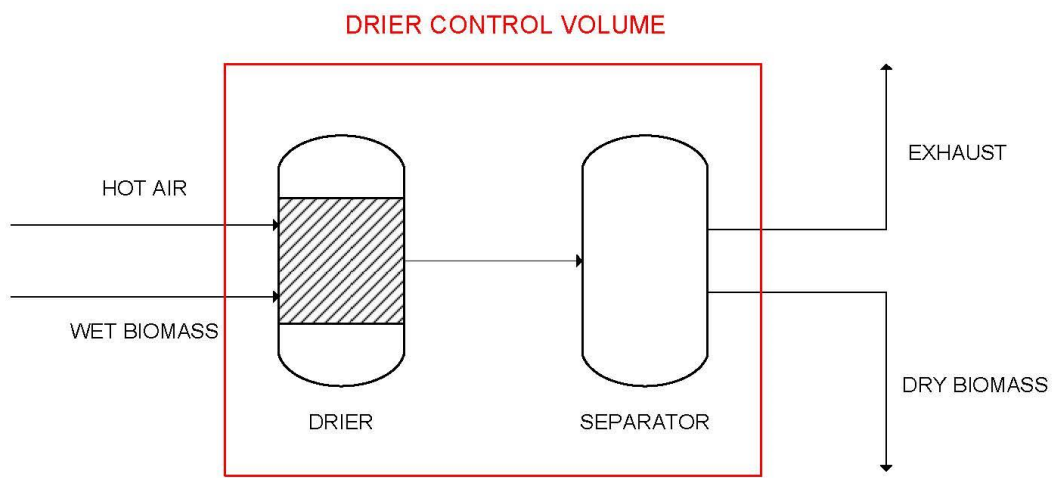


Figure 18 - Simulation model of biomass drying

Although biomass drying is not normally considered a chemical reaction, the effective drier is modelled with an RSTOIC block, in which a portion of the biomass reacts to form water. Since the RSTOIC block has a single outlet stream, a FLASH2 block has been used to separate the dried biomass from the moist air.

The equation that simulate the biomass drying is the following:



The drier block and the separator are supposed to be adiabatic and no pressure drops are considered. In a first moment, a temporary value of the fractional conversion of biomass is inserted, but this value will be overwritten by means of a Calculator Block.

Indeed, in order to handle the moisture content of the dried biomass, a Calculator Block is utilized. It allows to specify the moisture content of the dried biomass and to calculate the corresponding fractional conversion of biomass to water.

The fractional conversion is calculated considering the following mass balance equations applied to the moisture content and to the overall biomass:

$$\dot{m}_{wetbiomass} \cdot \frac{H_2O_{in}}{100} = \dot{m}_{drybiomass} \cdot \frac{H_2O_{out}}{100} + \dot{m}_{wetbiomass} \cdot CONV \quad Eq.26$$

$$\dot{m}_{wetbiomass} = \dot{m}_{drybiomass} + \dot{m}_{wetbiomass} \cdot CONV \quad Eq.27$$

where:

$\dot{m}_{wetbiomass}$ is the mass flow rate of the inlet biomass [kg/s];

$\dot{m}_{drybiomass}$ is the mass flow rate of the outlet biomass [kg/s];

H_2O_{in} is the weight percentage of moisture of the inlet biomass;

H_2O_{out} is the weight percentage of moisture of the outlet biomass;

$CONV$ is the fractional conversion of biomass to water.

Combining these two equations, it is possible to obtain an expression for the fractional conversion:

$$CONV = \frac{H_2O_{in} - H_2O_{out}}{100 - H_2O_{out}} \quad Eq.28$$

In this way, by imposing a weight percentage of moisture of the outlet biomass, it is possible to calculate the fractional conversion that will be assigned to the drier block.

3.3. Gasification section

Fig.19 shows the simulation model of the gasification section. The dried biomass exiting from the previous section is fed to the gasifier, together with the gasifying agent, while the final product is represented by the syngas. Analogously to the previous case, the simulation flowsheet uses two-unit operation blocks to simulate a single piece of equipment and the extra stream that connect the two simulation blocks, has not a real physical meaning.

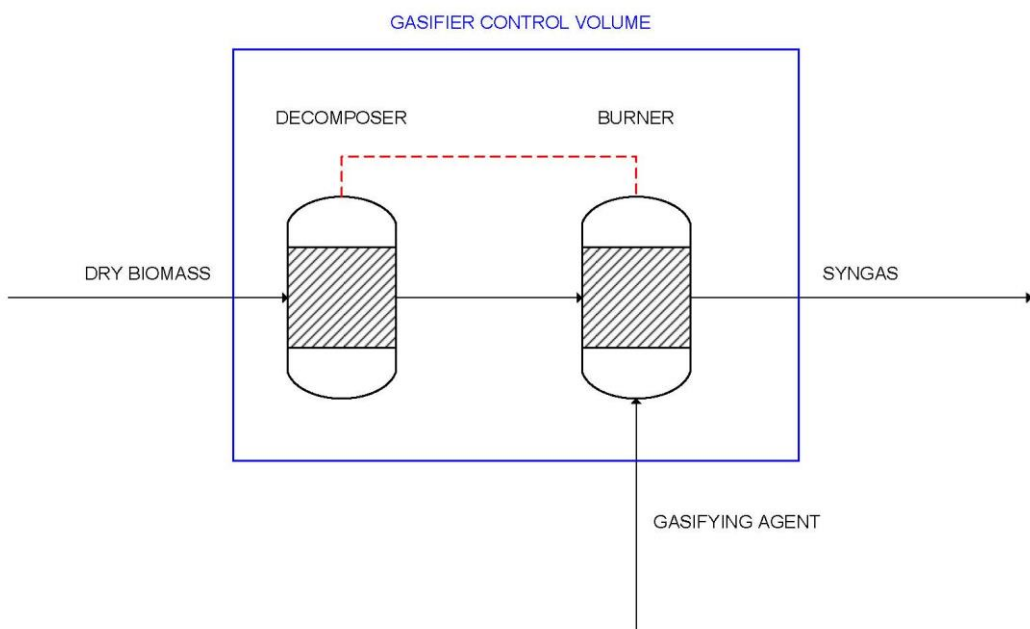


Figure 19 - Simulation model of the gasification section

The RGIBBS block has been utilized to simulate the gasification of the dry biomass. It models the chemical equilibrium by minimizing Gibbs free energy. However, the Gibbs free energy of the biomass cannot be calculated because it is a nonconventional component. Thus, the dried biomass needs to be decomposed into its constituent elements, before to be feed to the RGIBBS block. This is done by means of a RYIELD block. In order to ensure that the gasifier represents an auto-thermal system, the heat of reaction associated with the decomposition of biomass must be considered in the biomass gasification. Therefore, a heat stream has been used to carry this heat of reaction from the RYIELD block to the RGIBBS block.

RGIBBS block is used to model reactions that come to chemical equilibrium, since it calculates chemical equilibrium and phase equilibrium by minimizing the Gibbs free energy of the system. Therefore, it has not been needed to indicate the reactions that occur within a gasifier. Moreover, no pressure drops have been considered along the reactor.

However, assuming the equilibrium condition, the syngas composition will show a too low methane content, with respect to the effective syngas composition that can be found in literature [14]. Despite this fact, the hypothesis of equilibrium can be considered acceptable, being methane the final product of the whole plant.

By default, RGIBBS block assumes that all of the component defined at the beginning could be potential products in the vapour phase or the liquid phase. This default, anyhow, is not appropriate, since any carbon that remains after combustion would be solid and therefore a phase of pure solid must be assigned to it.

RYIELD block is used to simulate a reactor with a known yield and does not require any reactions. This reactor is supposed to be isothermal and no pressure drops have been considered along the reactor.

In a first moment, a temporary value of the yield distribution is inserted, but, again, this value will be overwritten by means of a Calculator Block.

Indeed, in order to calculate the effective yield distribution, the ultimate analysis has been converted to a wet basis, through the factor F:

$$F = \frac{100 - H_2O}{100} \quad \text{Eq.29}$$

where H_2O represents the moisture percentage of the dried biomass.

Hence, the effective yield distribution of the individual species in the decomposer block will be:

$$Y_{H_2O} = \frac{H_2O}{100} \quad \text{Eq.30}$$

$$Y_{ash} = \frac{ASH}{100} \cdot F \quad \text{Eq.31}$$

$$Y_C = \frac{C}{100} \cdot F \quad \text{Eq.32}$$

$$Y_{H_2} = \frac{H_2}{100} \cdot F \quad \underline{Eq.33}$$

$$Y_{N_2} = \frac{N_2}{100} \cdot F \quad \underline{Eq.34}$$

$$Y_{Cl} = \frac{Cl}{100} \cdot F \quad \underline{Eq.35}$$

$$Y_S = \frac{S}{100} \cdot F \quad \underline{Eq.36}$$

$$Y_{O_2} = \frac{O_2}{100} \cdot F \quad \underline{Eq.37}$$

where:

H_2O represents the moisture percentage of the dried biomass proximate analysis;

$ASH, C, H_2, N_2, Cl_2, S, O_2$ represent the percentages of the dried biomass ultimate analysis.

3.3.1. Gasification performances

There are some parameters that influence the performance of syngas production during gasification. They are, essentially, the types of gasifier and some operating conditions (such as equivalence ratio, steam-to-biomass ratio, type of biomass, type of gasifying agent). In this work, it has been chosen to fix some of them and to focus on the remaining ones, which have been investigated in order to design the best gasification system. In the following sections, these factors have been highlighted.

Influence of the equivalence ratio

The equivalence ratio is the main operating parameter that affects biomass gasification. This index represents the ratio between the mass of air under the actual operating conditions and the mass of air under stoichiometric conditions, or, equally, the ratio between the mass of oxygen under the actual operating conditions and the mass of oxygen under stoichiometric conditions. It is possible to distinguish different situations according its value: when the equivalence ratio is equal to one, stoichiometric combustion occurs, when it's larger than one, combustion in fuel lean conditions takes place and finally when it's less than one, fuel rich combustion happens.

Gasification, thus, represents a fuel rich combustion: typical equivalence ratio values range between 0,2 and 0,4. [15]

The mass of oxygen required for the combustion of a generic fuel under stoichiometric conditions is calculated considering that 1 kg of carbon needs 2,667 kg of oxygen, 1 kg of hydrogen needs 8 kg of oxygen and 1 kg of sulphur needs 1 kg of oxygen.

Therefore, known from the ultimate analysis the weight based percentages of these elements, it is possible to approximate the mass of oxygen required for the combustion of a generic fuel under stoichiometric conditions:

$$O_{2,stoic} = 2,667 \cdot C + 8 \cdot H + S - O$$

Eg.38

where C, H, S and O are the weight based percentages of the corresponding elements.

Through some sensitivity analysis, it has been investigated how the temperature and the composition of the output syngas vary by varying the equivalence ratio.

The following graphs have been obtained supposing beech as input biomass, with a steam-to-biomass ratio of 0.4, and a temperature of the gasifying agent (steam and oxygen) of 400 °C. Moreover, it has been considered that the drying section reduces the moisture content of the different biomasses to the 8%.

As it can be observed, with increasing of equivalence ratio, temperature increases. It is probably due to the major occurrence of the exothermic reactions, because of the injection of more oxygen into the system.

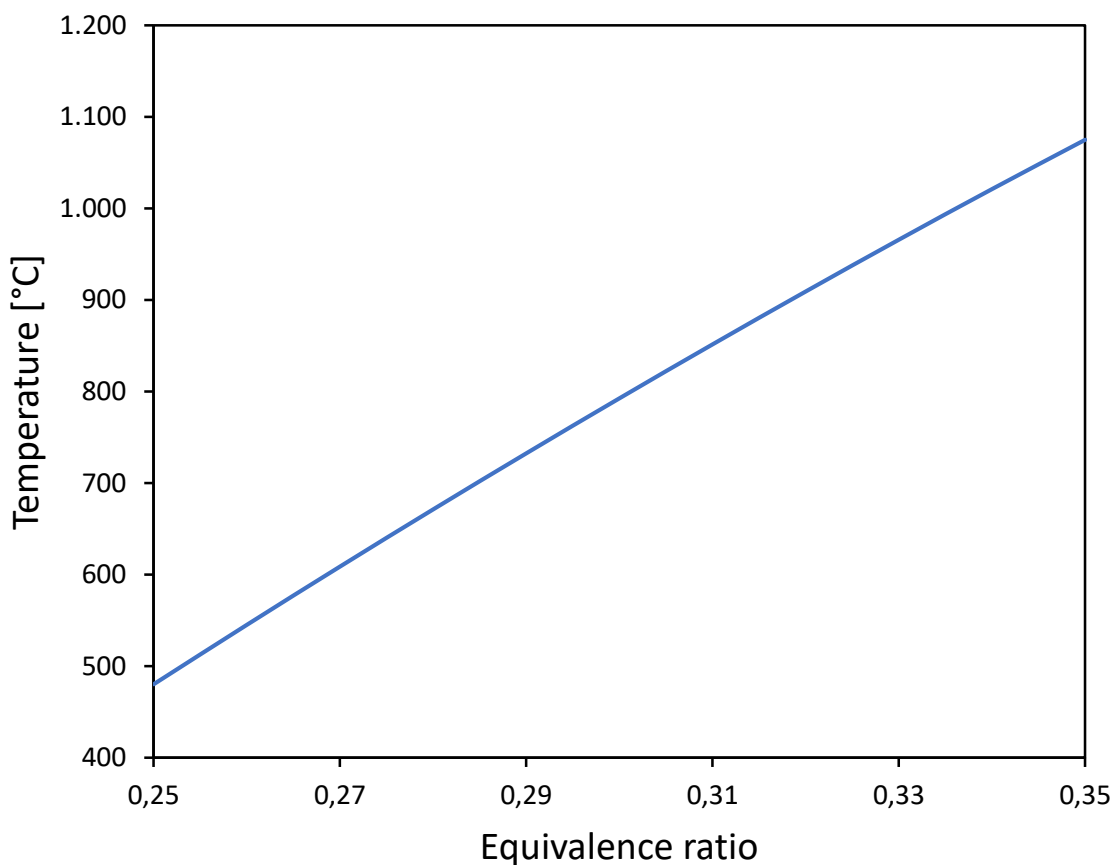


Figure 20 - Effects of equivalence ratio on temperature of gasification

Moreover, it is also shown that increasing the equivalence ratio leads to decreasing the H₂ content. It is probably due to the further occurrence of hydrogen oxidation, because of, again, the presence of more oxygen in the system, that consequently leads to the increasing of the H₂O content.

CO content of the final syngas, likewise, decreases by increasing the equivalence ratio while, as consequence, CO₂ content shows the inverse trend. Reducing the amount of carbon monoxide associated with a higher equivalence ratio value can be motivated by the fact that, with a higher equivalence ratio value, more oxygen is introduced and there should be more carbon monoxide converted, through oxidation, in carbon dioxide.

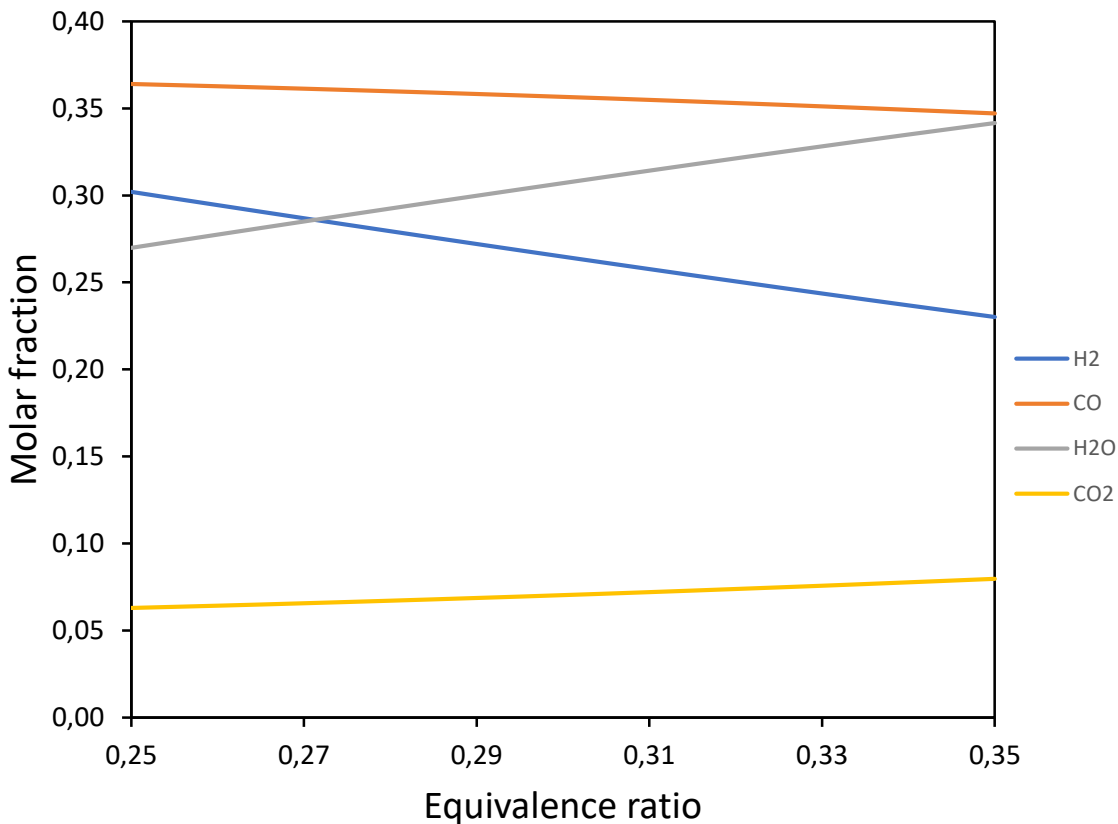


Figure 21 - Effects of equivalence ratio on syngas composition

Influence of the steam-to-biomass ratio

When steam is used as a gasification agent, steam-to-biomass ratio, which represents the mass ratio between steam and biomass, is another important parameter. It represents the ratio between the mass flow rate of steam used as gasifying agent and the mass flow rate of the inlet biomass.

The influence of the steam to biomass ratio on the temperature of gasification and on the composition of the final syngas has been investigated.

The following graphs have been obtained supposing beech as input biomass, with an equivalence ratio of 0.4, and a temperature of the gasifying agent (steam and oxygen) of 400 °C. Moreover, it has been considered that the drying section reduces the moisture content of the different biomasses to the 8%.

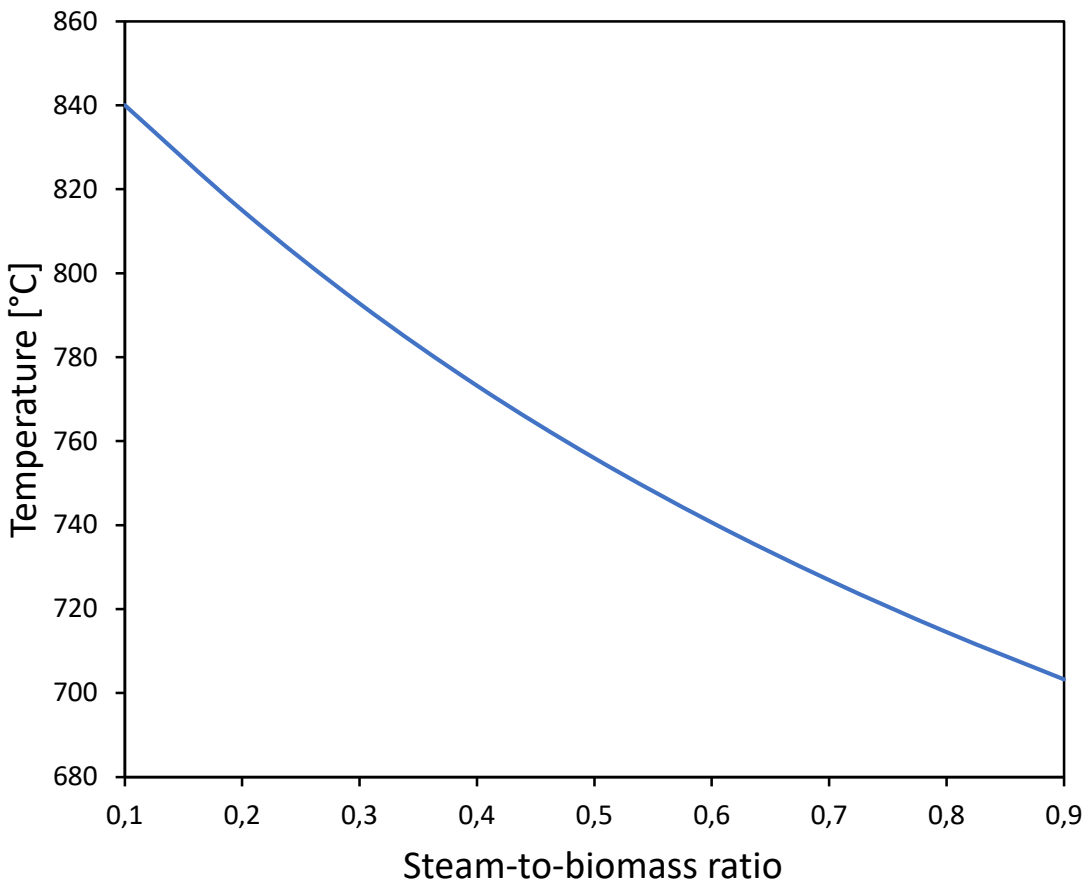


Figure 22 - Influence of steam-to-biomass ratio on temperature of gasification

The excessive increase of steam leads to a reduction in reaction temperature, which thus leads to a decrease in hydrogen. However, the increase in the values of the steam to biomass ratio lead to the increase in carbon dioxide but also to a steep decrease of the carbon monoxide, leading to a general increase of the H₂/CO.

Higher steam-to-biomass ratio means high water content in the produced. As known, the separation of the steam from produced gas can be easily carried out by condensation and dryness. However, more energy was consumed to produce excess steam as well as consumed in the process of condensation. So, it may be necessary to select an optimal steam/biomass ratio according to different operating condition.

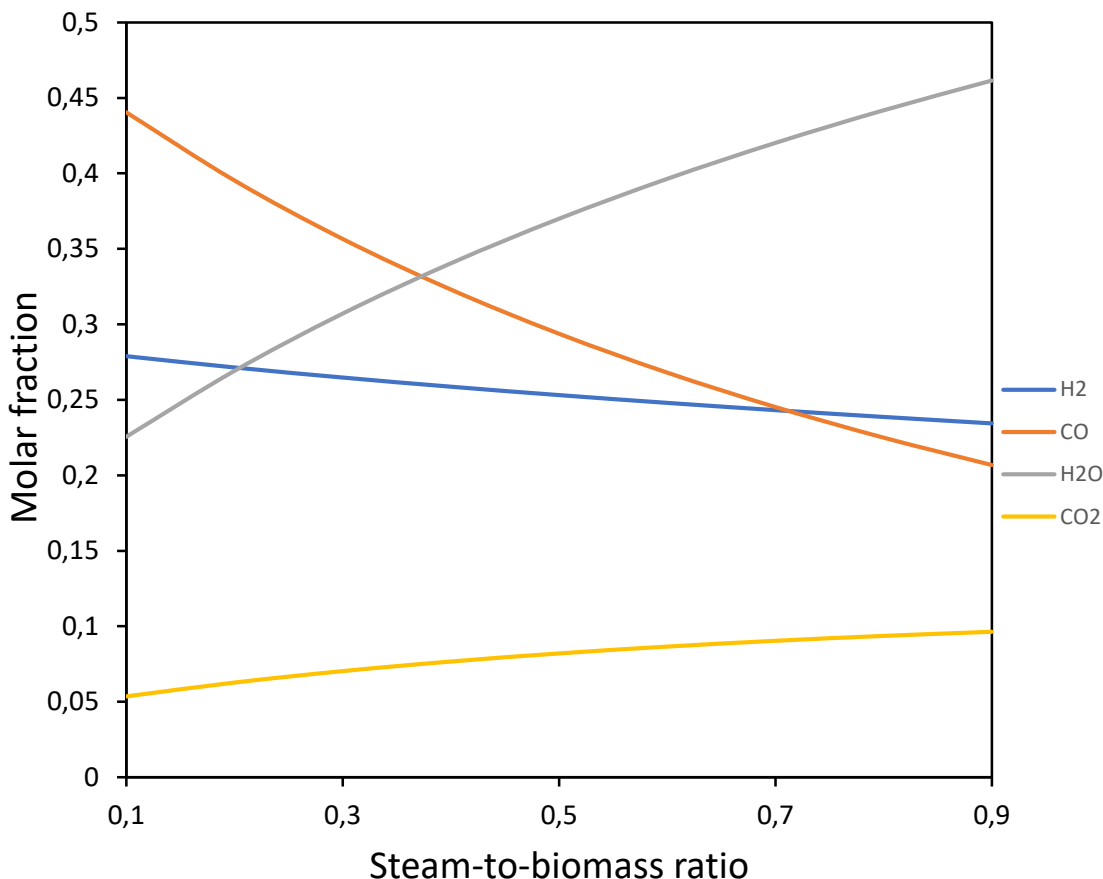


Figure 23 - Influence of steam-to-biomass ratio on syngas composition

Influence of the type of biomass

The 2009/28/EC European directive defines as “the biodegradable fraction of products, waste and residues of biological origin from agriculture (including vegetal and animal substances), forestry and related industries, including fisheries and aquaculture, as well as the biodegradable fraction of industrial and municipal wastes”. Biomasses diversify for various parameters such as moisture content, chemical composition, ashes and inorganic substances content and heat of combustion, leading to variations of the produced heat energy and composition of the final product. Thus, the knowledge of biomass physical-chemical properties is fundamental for its use as sustainable resource for energy production.

In this work, it has been investigated the temperature of gasification and the chemical species composition of the syngas exiting the gasifier, under determinate operating conditions, for five types of biomass: bark, beech, miscanthus, pine and rice straw.

		Bark	Beech	Miscanthus	Pine	Rice straw
Proximate analysis, weight %	Moisture (wet basis)	10,90	15,20	9,10	10,30	11,73
	Fixed Carbon (dry basis)	19,60	14,53	10,09	10,80	14,23
	Volatile Matter (dry basis)	78,10	84,87	86,50	82,80	65,62
	Ash (dry basis)	2,30	0,60	3,41	6,40	20,15
Ultimate analysis, weight %	C (dry basis)	55,10	49,38	48,60	51,57	39,24
	H (dry basis)	6,30	6,17	6,00	6,75	4,97
	N (dry basis)	0,44	0,28	0,52	0,29	1,27
	S (dry basis)	0,05	0,01	0,20	0,01	0,10
	O (dry basis)	35,8	43,55	41,07	34,97	33,64
	Cl (dry basis)	0,01	0,01	0,20	0,01	0,63
	Ash (dry basis)	2,30	0,60	3,41	6,40	20,15
Higher heating value [MJ/kg]		22,67	19,32	19,12	19,46	14,74

Table 2 - Properties of the investigated biomasses

The proximate and ultimate analysis and the heat of combustion of the selected biomass types are taken from Phyllis2 [16], which is a database containing information on the composition of biomass and waste, and are presented in Table 2.

The simulations have been carried out with an equivalence ratio of 0,3, a steam-to-biomass ratio of 0,3 and a temperature of the gasifying agent (steam and oxygen) of 350 °C. Moreover, it has been considered that the drying section reduces the moisture content of the different biomasses to the 8%.

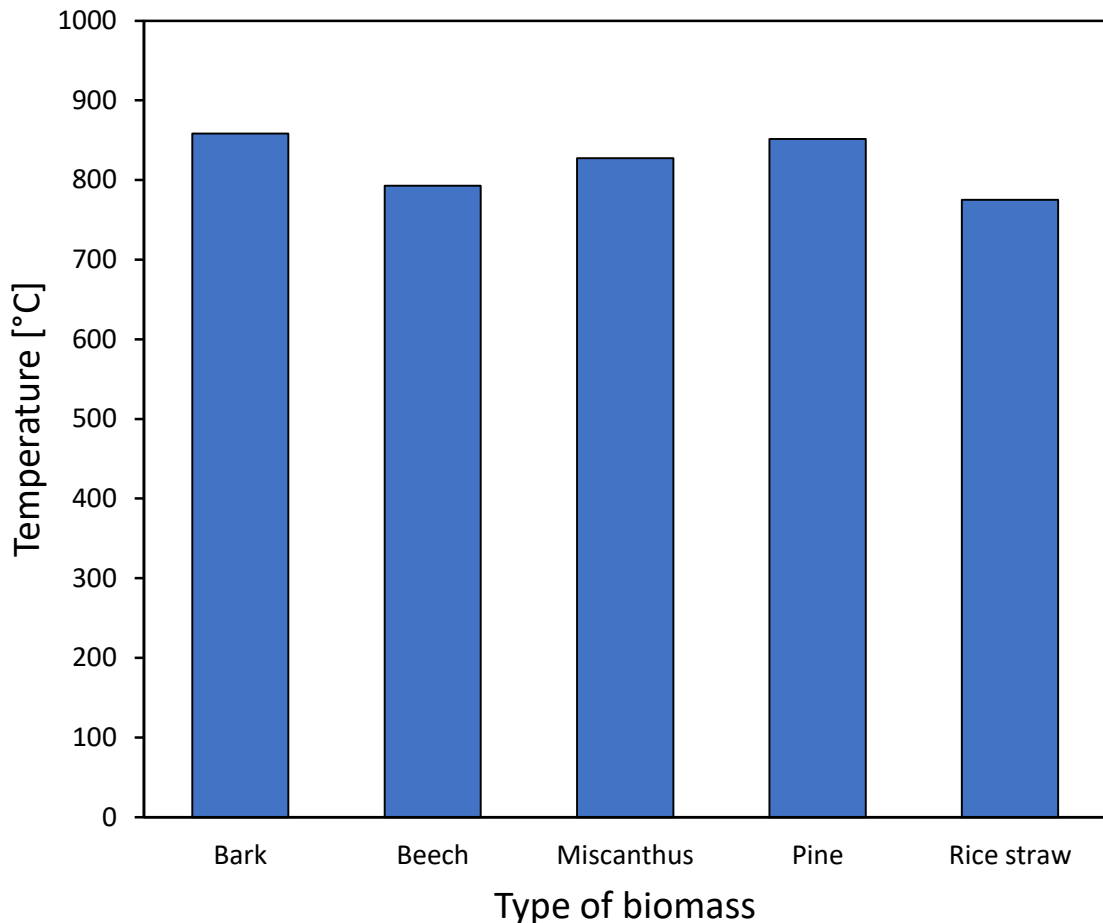


Figure 24 - Influence of the type of biomass on temperature of gasification

As it possible to see in Fig.24, the type of biomass modestly influences the gasification temperature, with the only exception of rice straw, which is characterized by a low heat of combustion and a high ash content with respect to the other biomasses analyzed.

However, the temperature of gasification ranges between 750°C and 850°C.

For what concerns the composition of the final product, reported in Fig.25, great differences can't be noted.

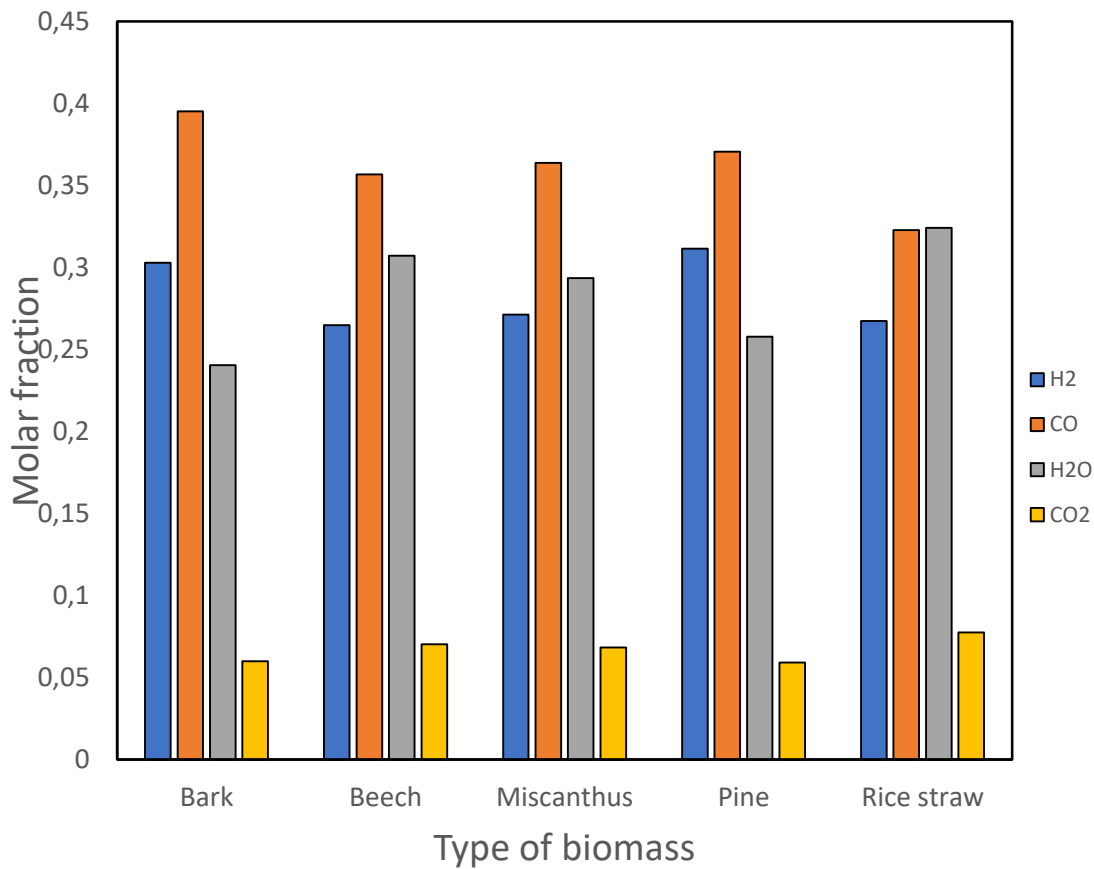


Figure 25 - Influence of the type of biomass on syngas composition

Influence of the temperature of the gasifying agent

Different gasifying agents, such as air, oxygen and steam or mixtures of these components, have been used for biomass gasification.

Air is the cheapest gasifying agent but it contains more than 75% in volume of nitrogen, that will dilute the syngas produced and absorb a substantial amount of heat, causing the decrease of the temperature of gasification and of the ratio H₂/CO. As a result, the syngas produced cannot be directly used for the production of many synfuels.

To some extent, utilization of oxygen-rich air or pure oxygen as the gasifying agent can overcome the limitations arising from the use of air. However, pure oxygen is extracted by means of very expensive processes and this fact could discourage its use.

Moreover, the use of steam as gasifying agent can improve the quality and the H₂/CO of the syngas produced. Nonetheless, a steam generator with reliable performance becomes necessary, which leads to additional equipment cost.

In this work, a mixture of steam and pure oxygen, which represent the outlet stream of the anode of the SOEC, is used as gasifying agent.

However, a sensitivity analysis has been performed, in order to understand how the temperature of gasification and the composition of the syngas produced change by varying the temperature of such gasifying agent. In the simulation performed using beech as input biomass, an equivalence ratio of 0,3 and a steam-to-biomass ratio of 0,35 have been fixed. Moreover, it has been considered that the drying section reduces the moisture content of the different biomasses to the 8%.

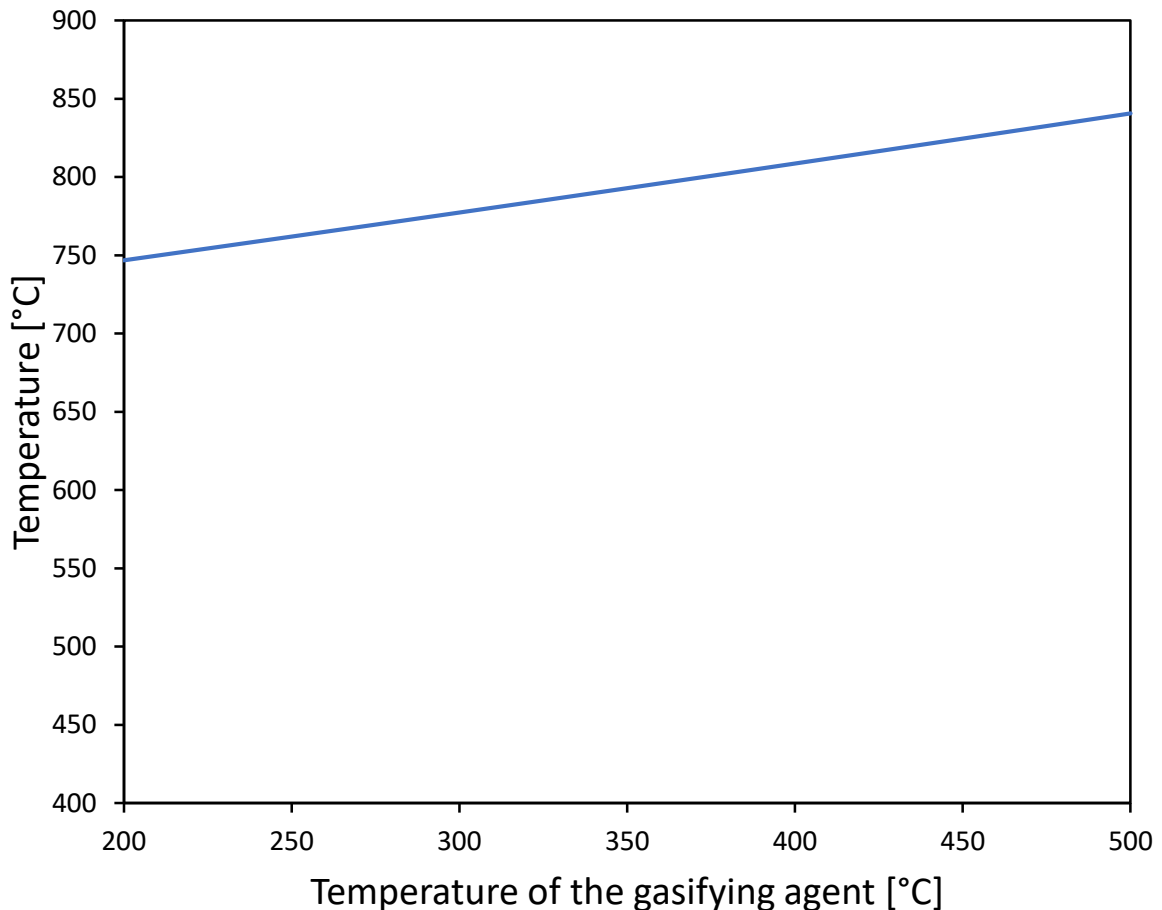


Figure 26 - Effect of the temperature of the gasifying agent on the temperature of gasification

As it is possible to see from Fig.26, a modest increase of the temperature of gasification corresponds to an increasing of the temperature of the gasifying agent. On the contrary, the temperature of the gasifying agent does not affect at all the composition of the final syngas, and this is clearly shown in Fig.27.

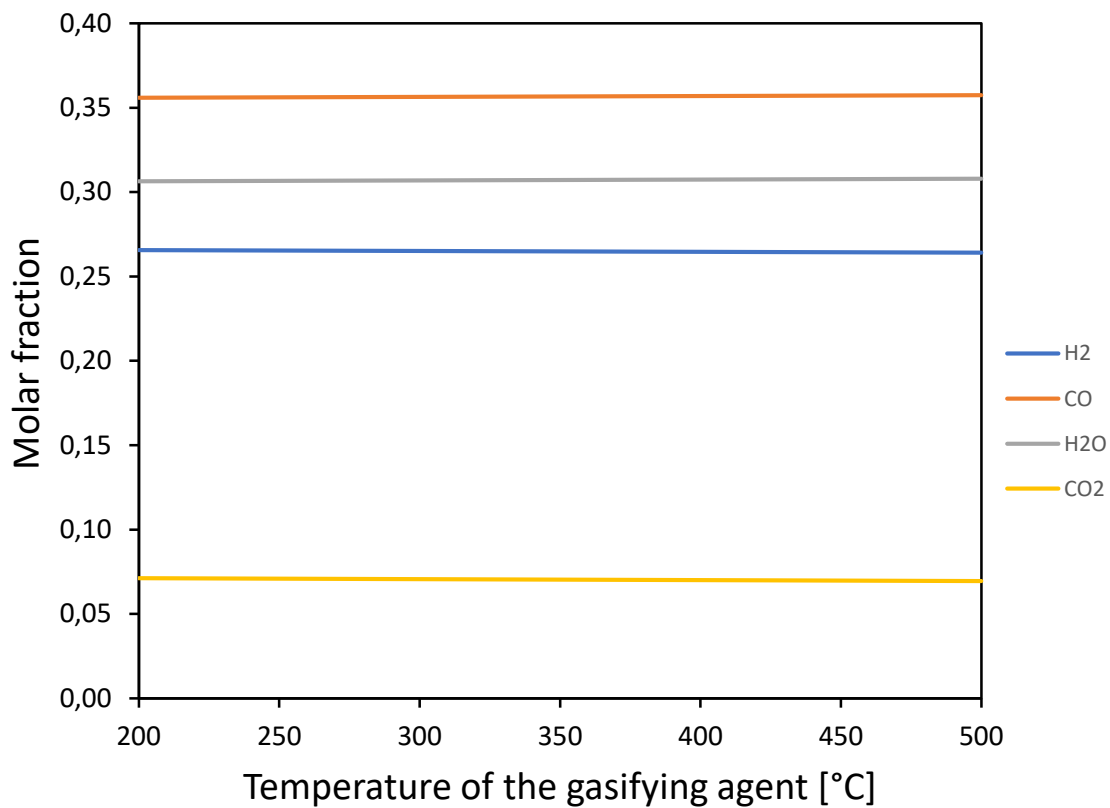


Figure 27 - Effect of the temperature of the gasifying agent on the composition of the syngas produced

3.4. Methanation line

The simulation model of the methanation line is shown in Fig.28. The syngas produced in the gasification process, cleaned of the contaminants, separated from the water and enriched with the hydrogen coming from the water electrolysis, enters into the system. The synthetic natural gas and the water coming from the reaction of methanation of carbon monoxide and dioxide, exit from the system.

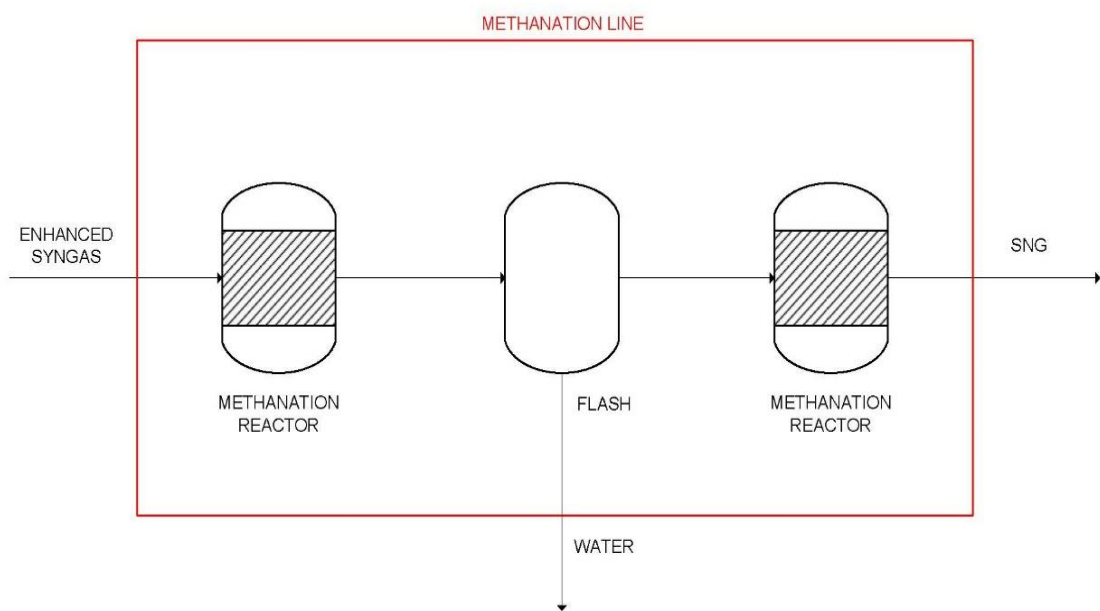


Figure 28 - Simulation model of the methanation line

Once again, the RGIBBS block has been employed in order to simulate the behaviour of a methanation reactor. As already mentioned, it is used to model reactions that come to chemical equilibrium, since it calculates chemical equilibrium and phase equilibrium by minimizing the Gibbs free energy of the system. Therefore, it has not been needed to indicate the reactions that occur within a gasifier. Moreover, no pressure drops have been considered along the reactor.

In order to reach high methane concentrations (95-98%), the chosen methanation concept consists of a series of two cooled reactors with an intermediate condensation stage in order to remove the produced water. This configuration has been preferred to a more conventional one with adiabatic reactors because the outlet adiabatic temperature within the first reactor could reach too-high values. Such a high temperature can lead to nickel sintering or, more generally, to catalyst structural

damages. In order to ensure the proper heat transfer between reacting gas and coolant, a “shell-and-tube” reactor has been considered for methanation: tubes are filled with catalyst packed pellets, while in the shell the coolant circulation takes place. Considering the thermal coupling between exothermal methanation and steam production (required since the synthetic gas production system is integrated with high temperature steam electrolysis), evaporating (saturated) water has been chosen as the cooling fluid. [17]

Downstream methanation of the syngas is carried out to yield a stream of almost pure methane that is suitable (in terms of composition and heating value) to be injected into the natural gas grid.

3.5. Solid oxide electrolytic cell unit

Fig.29 shows the simulation model of the solid oxide electrolytic cell unit. It uses two-unit operation blocks to simulate a single piece of equipment and, for this reason, the extra stream that connect the two simulation blocks has not a real physical meaning. Moreover, it is important to note that, from it, there is no clear distinction between anode and cathode of the SOEC. Hot steam enters into the system, standing for both cathode inlet stream and anode (sweep gas) inlet stream. A mixture of hydrogen and steam, which stands for the cathode outflow, and a mixture of oxygen and steam, which stands for the anode outflow, exit from the system.

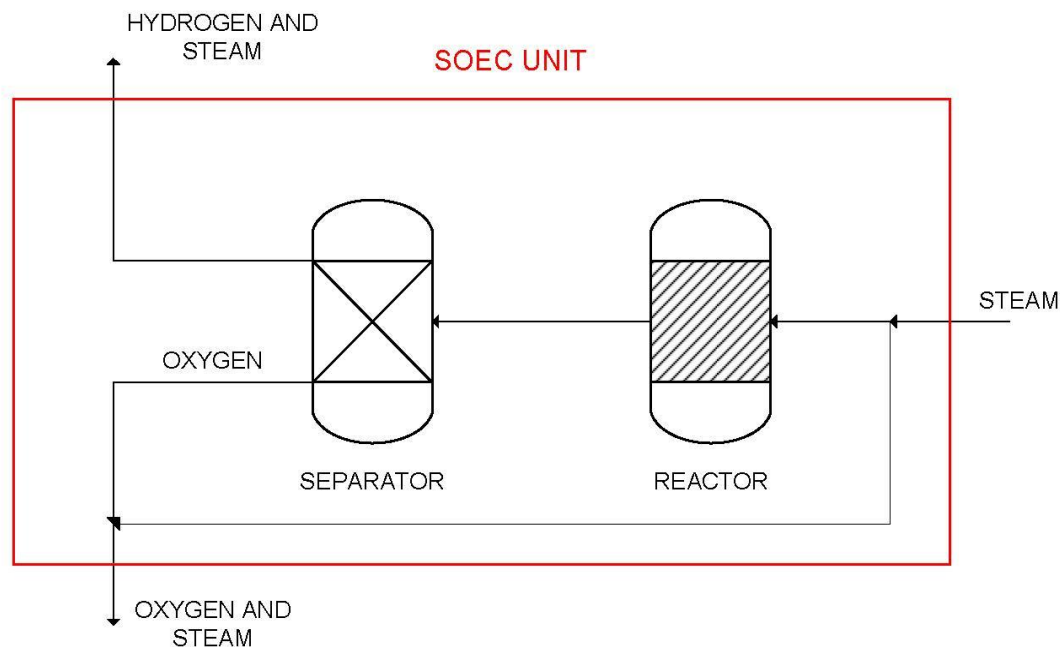


Figure 29 - Simulation model of the solid oxide electrolytic cell unit

The RSTOIC block has been used in order to simulate the overall reaction of water electrolysis. It is used when stoichiometry and the molar extent or conversion is known for each reaction that takes place. It can model reactions occurring simultaneously or sequentially. So the reaction occurring and a fractional conversion have been specified. The reactor operates at a constant temperature and no pressure drops have been considered along the reactor.

In order to separate the products of the reaction of water electrolysis, a separator block has been used. Its task is to separate the hydrogen and the remaining water from the oxygen, to which the sweep gas flow is added. In fact, to ensure that the steam used as a gas sweep does not participate in the electrolysis reaction, it is added to the oxygen flow only at the end of the reaction.

3.6. Rankine cycle

The simulation model of the Rankine cycle is shown in Fig.30. It consists in a closed loop in which water is firstly pumped from low to high pressure and then becomes overheated steam by means of a steam generator, where it is heated at constant pressure. The overheated steam expands through a turbine, generating power, and finally is condensed at constant pressure.

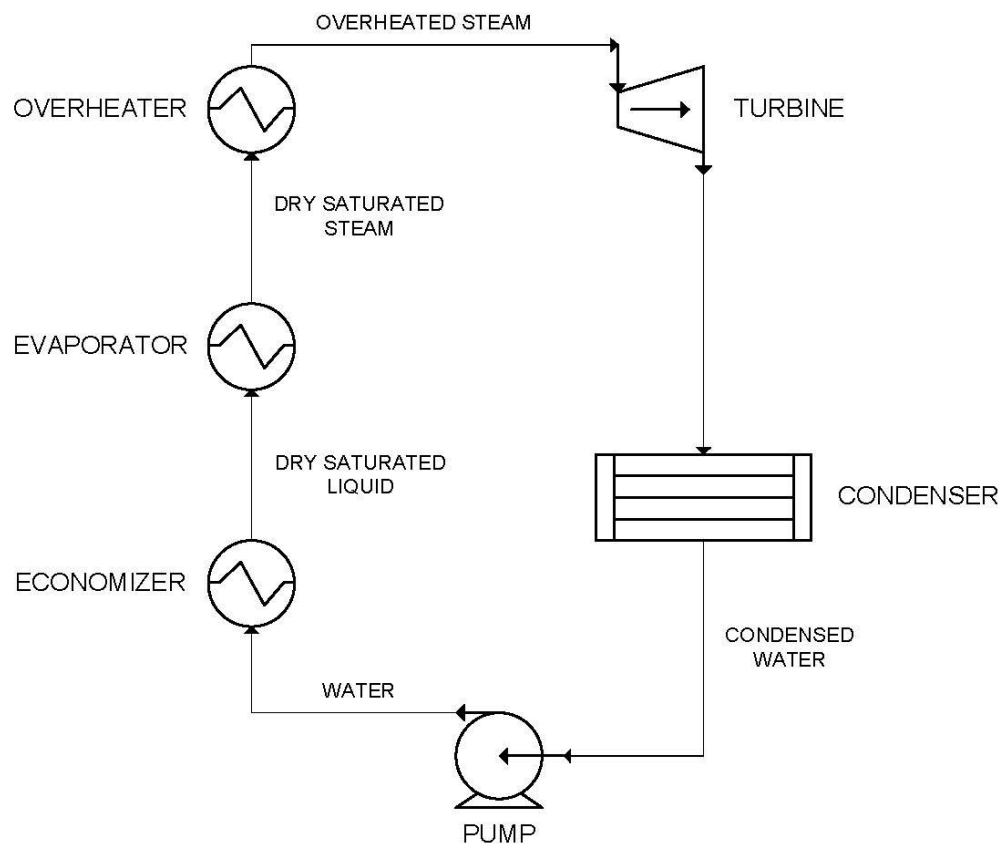


Figure 30 - Simulation model of the Rankine cycle

The steam generator has been modelled using three heat exchangers, standing for economizer, evaporator and overheater. All these heat exchangers operate at constant pressure. In order to simulate the behaviour of the economizer, in the first heat exchanger it has been imposed the target of degrees of subcooling equal to 0, while in order to simulate the behaviour of the evaporator, in the second heat exchanger it has been imposed the target of degrees of superheating equal to 0. The temperature of overheating is the result of the thermal integration analysis.

The turbine has been modelled as an isentropic turbine and thus an isentropic efficiency of 0,8 and a mechanical efficiency of 0,98 have been imposed, as well as a certain discharge pressure.

Finally, the condenser has been modelled using a heat exchanger that returns the turbine output flow to the pump entry conditions.

4. Process integration and efficiency

4.1. Process integration

After describing the single sections in detail, it has been proceeded with the process integration. In particular, two different plant configurations have been examined. Both provide for the integration of all the sections described above, but the substantial difference lies in the sizing of the SOEC. In the first configuration, it is sized so to provide the syngas with the amount of hydrogen necessary to match the requirement of the methanation reactor, which is:

$$FEED = \frac{y_{H_2} - y_{CO_2}}{y_{CO} + y_{CO_2}} = 3 \quad \text{Eq. 24}$$

In the second configuration, it is sized so as to provide the gasifier with the desired amount of gasifying agent. Therefore, to match the requirement of the methanation, a water gas shift (WGS) reactor and a carbon dioxide capture and sequestration (CCS) section have been inserted.

The two process configurations have been designed with the same gasification conditions, i.e. same type of biomass, same biomass flow, same equivalence ratio and same steam-to-biomass ratio.

The following table shows the gasification conditions adopted in the design of the two system configurations.

Property	Value
Type of biomass	Beech
Mass flow rate of biomass [kg/s]	0,5
Equivalence ratio	0,3
Steam-to-biomass ratio	0,196

Table 3 - Gasification conditions for both configurations of the plant

In particular, beech has been chosen as type of biomass since it is a biomass of recent interest according to Brisk2, which is a European project whose main activity is to fund researchers to access biological and thermal biomass conversion facilities across Europe. The value of the equivalence ratio has been chosen because it guarantees a gasification temperature high enough so that the equilibrium hypothesis is respected.

The value of the steam-to-biomass ratio is bound to the value of equivalence ratio because the anode output flow is a mixture of oxygen and steam and thus it is possible to manage only one of the ratios. It has been chosen to manage the equivalence ratio since it is the parameter that influences more the gasification performance.

Finally, the temperature of the gasifying agent, which is the only parameter different for the two configurations, is the result of the thermal integration, that will be described in the following pages.

For both configurations, a separator simulates the syngas cleaning, which has been described in the technology overview but does not have an energy cost.

4.1.1. First configuration

A detailed flowsheet of the first configuration plant is reported in Fig.31. The wet biomass enters to the drying section, in which the drying is performed through hot air. The dried biomass, whose moisture content were reduced to 8%, enters to the gasifier where gasification process takes place by using a mixture of pure oxygen and steam, representing a part of the anode output flow. The syngas produced is firstly cooled, so as to allow the separation of water, and then enriched with the hydrogen coming from the cathode of the SOEC, which permits to adjust the ratio of the syngas before the subsequent methanation reactor.

The mass flow rate of the steam entering to the SOEC has been set by means of a Design Specification, which is a tool of Aspen Plus™. It allows to calculate the value of a certain variable which guarantees the achievement of the value of a fixed variable, with a tolerance that must be specified. The lower the tolerance value, the higher the computational cost of using this tool. In particular, through a Fortran statement, it has been calculated the value of the mass flow rate of the steam entering to the SOEC that allows to match the requirement of the syngas entering the methanation section, with a tolerance of 0,001.

The molar flow rate of the steam used as sweep gas, instead, has been chosen so that it has the same order of magnitude as that of the oxygen produced by the SOEC.

Moreover, before the methanation reactor, an isentropic compressor increases the pressure of the enhanced syngas up to 16 bar because methanation reaction is favoured at high pressures according to Le Châtelier principle (being a reaction with decreasing number of moles). For the compressor, an isentropic efficiency of 0,8 and a mechanical efficiency of 0,98 has been fixed.

After having been compressed, the enhanced syngas is heated up to the temperature of 285°C and enters to the methanation section, where the SNG is produced.

Finally, the excess mass flow rate of steam that will feed the Rankine cycle corresponds to the mass flow rate of the excess evaporating saturated water used as cooling fluid in the “shell-and-tube” methanation reactors. The pressure at which the overheated steam is produced has been fixed to 40 bar. In this way, the corresponding temperature of evaporation will be roughly 250°C, allowing a good coupling with the methanation reactors.

The temperature of the overheated steam has been calculated through another design specification. It represents the temperature that allows not to reach a vapour fraction of the stream leaving the turbine lower than 0,95 at the discharge pressure of the turbine, which has been set equal to 0,05 bar. Having a vapour fraction lower than 0,95

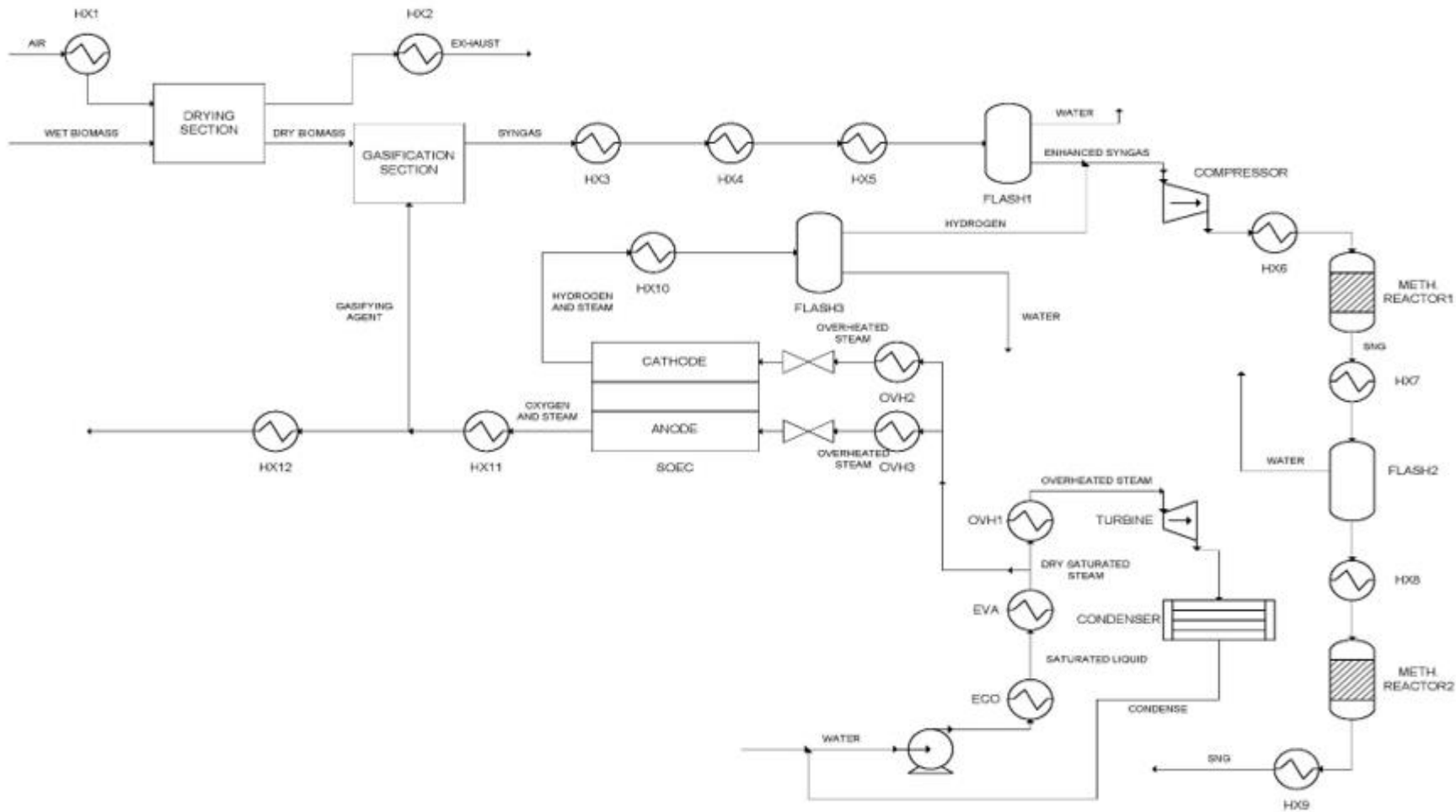


Figure 31 - Detailed flowsheet of the first configuration of the plant

would damage in an irreparable way the blades of the turbine. Also in this case, a tolerance of 0,001 has been set.

Table 4 reports the main streams of the configuration with some of their properties such as pressure, temperature, mass flow rate, enthalpy and molar composition in terms of nitrogen, oxygen, water, hydrogen, carbon monoxide, carbon dioxide and methane.

Stream	Pressure [bar]	Temperature [°C]	Mass flow rate [kg/s]	Enthalpy [kJ/kg]	Molar composition						
					N ₂	O ₂	H ₂ O	H ₂	CO	CO ₂	CH ₄
Beech	1	15	0,5	-7213	-	-	-	-	-	-	-
Dried beech	1	292,22	0,46087	-5843	-	-	-	-	-	-	-
Air	1	15	3	-10	0,79	0,21	-	-	-	-	-
Exhaust	1	15	3,03913	-188	0,774	0,206	0,020	-	-	-	-
Gasifying agent	1	495,4	0,272656	-4182	-	0,502	0,498	-	-	-	-
Cleaned syngas	1	968,16	0,729587	-5249	-	1e-4	0,268	0,271	0,399	0,062	6e-11
Enhanced syngas	16	285	0,677697	-3804	-	5e-5	0,032	0,734	0,203	0,031	3e-11
SNG	1	15	0,285454	-4875	-	-	0,019	0,012	6e-7	0,002	0,967
Water SOEC	1	15	0,939386	-16017	-	-	1	-	-	-	-
Steam SOEC	1	800	0,939386	-11810	-	-	1	-	-	-	-
Water sweep	1	15	0,396336	-16017	-	-	1	-	-	-	-
Steam sweep	1	800	0,396336	-11810	-	-	1	-	-	-	-
Water Rankine	1	15	0,712086	-16017	-	-	1	-	-	-	-
HP steam Rankine	40	524,768	0,712086	-12475	-	-	1	-	-	-	-
LP steam Rankine	0,05	36,0331	0,712086	-13529	-	-	1	-	-	-	-
Anode outlet	1	800	1,10547	-3728	-	0,502	0,498	-	-	-	-
Cathode outlet	1	800	0,230256	-2821	-	-	0,15	0,85	-	-	-

Table 4 - Main streams of the first configuration of the plant

4.1.2. Second configuration

A detailed flowsheet of the first configuration plant is reported in Figure 32. The wet biomass enters to the drying section, in which the drying is performed through hot air. The dried biomass, whose moisture content were reduced to 8%, enters to the gasifier where gasification process takes place by using a mixture of pure oxygen and steam, which represents the cathode outlet.

Indeed, through a Design Specification it has been calculated the mass flow rate of steam that guarantees the reaching of an equivalence ratio of 0,3, with a tolerance of 0,001. The molar flow rate of the steam used as sweep gas, instead, has been chosen so that it has the same order of magnitude as that of the oxygen produced by the SOEC.

However, operating in this way, the hydrogen produced by the SOEC will not be sufficient in order to match the requirement of the methanation. For this reason, a water gas shift reactor and a carbon capture section are required.

The water gas shift reactor has been modelled using a REQUIL block. It can be used when the reactions involved are equilibrium reactions. Differently from the other reactor blocks, REQUIL block has a vapour and liquid phase product streams and both are required. It operates at a constant temperature of 250°C and no pressure drops have been considered along the reactor.

Thus, the syngas exiting from the gasifier is firstly cooled until 250°C and then enters the water gas shift reactor. The reaction needs a molar flow rate of steam equal to the molar flow rate of carbon monoxide, but the steam already present in the syngas is not sufficient to satisfy the requirement. For this reason, additional steam is required for the reactor and this quantity is calculated by means of a Calculator Block.

The syngas exiting from the water gas shift reactor enters to the carbon capture section where a certain amount of carbon dioxide is captured. This section is modelled simply using a separator block and a splitter. Obviously, this is a considerable simplification since a carbon capture plant has a high degree of complexity, but in this way it is possible to do not burden further the flowsheet. The separator block divides all the carbon dioxide, while the splitter recirculates a part of the carbon dioxide separated in order to match the requirement of the methanation reactor. This is done by means of a Design Specification, through which it is calculated the split fraction to recirculate the carbon dioxide that adjust the ratio before the methanation. A tolerance of 0,001 has been set.

Before the methanation reactor, an isentropic compressor increases the pressure of the enhanced syngas up to 16 bar because methanation reaction is favoured at high pressures according to Le Châtelier principle (being a reaction with decreasing number

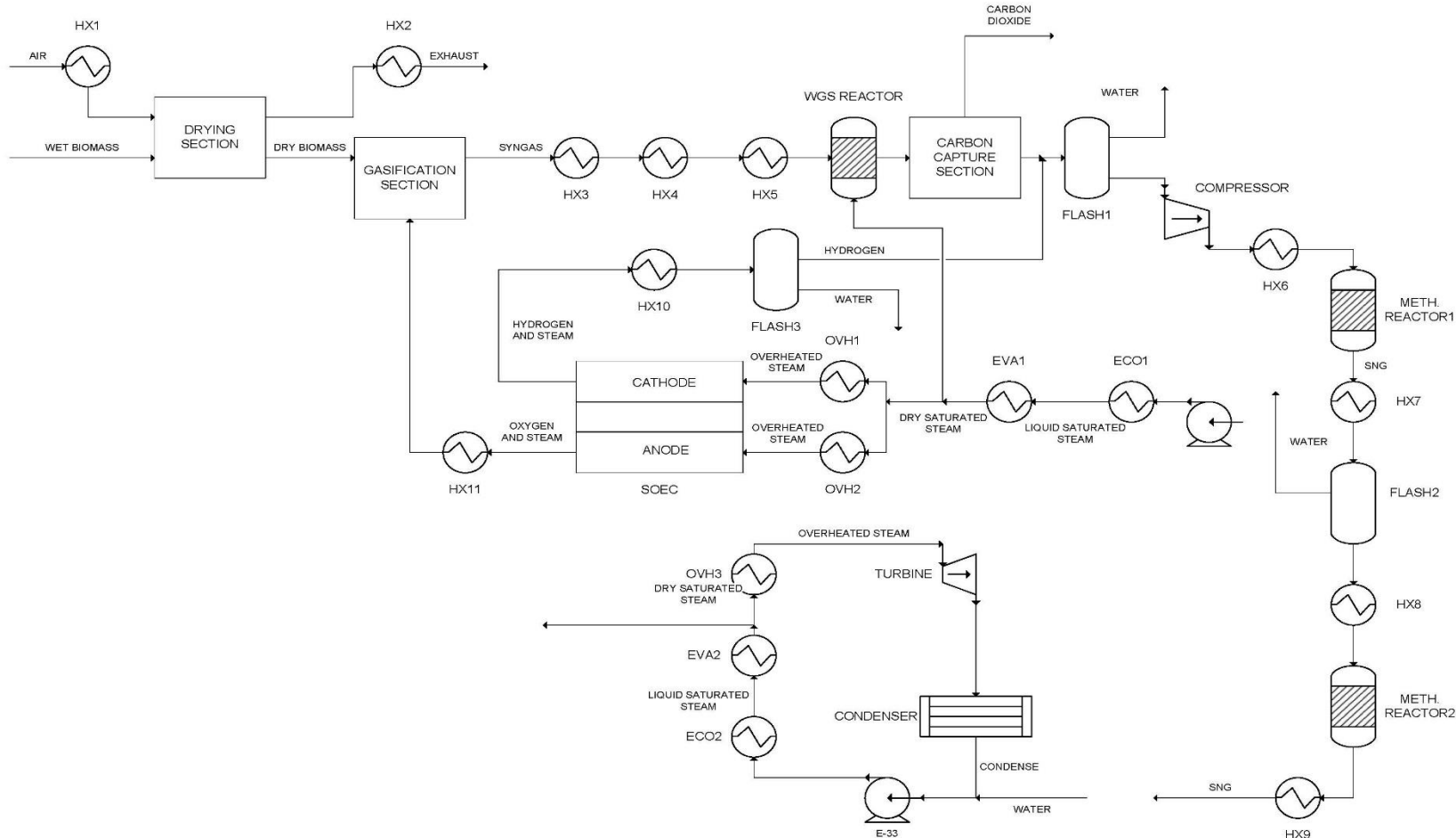


Figure 32 - Detailed flowsheet of the second configuration of the plant

of moles). For the compressor, an isentropic efficiency of 0,8 and a mechanical efficiency of 0,98 has been fixed.

After having been compressed, the enhanced syngas is heated up to the temperature of 285°C and enters to the methanation section, where the SNG is produced.

Finally, a Rankine cycle whose steam generator is fed with excess heat due to the cooling of the syngas, is used to produce an extra amount of power.

Table 5 reports the main streams of the configuration with some of their properties such as pressure, temperature, mass flow rate, enthalpy and molar composition in terms of nitrogen, oxygen, water, hydrogen, carbon monoxide, carbon dioxide and methane.

Stream	Pressure [bar]	Temperature [°C]	Mass flow rate [kg/s]	Enthalpy [kJ/kg]	Molar composition						
					N ₂	O ₂	H ₂ O	H ₂	CO	CO ₂	CH ₄
Beech	1	15	0,5	-7213	-	-	-	-	-	-	-
Dried beech	1	220,02	0,46087	-6029	-	-	-	-	-	-	-
Air	1	15	1,5	-10	0,79	0,21	-	-	-	-	-
Exhaust	1	15	1,53913	-388	0,758	0,202	0,040	-	-	-	-
Gasifying agent	1	496,11	0,272178	-4167	-	0,503	0,497	-	-	-	-
Cleaned syngas	1	908,03	0,72911	-5361	-	1e-4	0,268	0,271	0,399	0,062	6e-11
Carbon dioxide	1	250	0,368068	-8728	-	-	-	-	-	1	-
Enhanced syngas	16	285	0,471002	-6578	-	9e-5	0,042	0,757	0,044	0,156	5e-11
SNG	1	15	0,149557	-4932	-	-	0,022	0,018	4e-7	0,003	0,956
Steam WGS	1	250	0,089263	-12993	-	-	1	-	-	-	-
Water SOEC	1	15	0,231685	-16017	-	-	1	-	-	-	-
Steam SOEC	1	800	0,231685	-11810	-	-	1	-	-	-	-
Water sweep	1	15	0,097282	-16017	-	-	1	-	-	-	-
Steam sweep	1	800	0,097282	-11810	-	-	1	-	-	-	-
Water Rankine	1	15	0,155	-16017	-	-	1	-	-	-	-
HP steam Rankine	40	675,474	0,155	-12129	-	-	1	-	-	-	-
LP steam Rankine	0,05	58,0944	0,155	-13361	-	-	1	-	-	-	-
Steam CCS	1	250	0,1243	-12992	-	-	1	-	-	-	-
Cathode outlet	1	800	0,056789	-2821	-	-	0,15	0,85	-	-	-

Table 5 - Main streams of the second configuration of the plant

4.2. Thermal integration

In order to perform the thermal integration, the methodology of pinch analysis has been applied to both the configurations. Pinch analysis is a methodology for reducing energy consumption of processes by calculating thermodynamically feasible energy targets (or minimum energy consumption) and achieving them by optimizing heat recovery systems, energy supply methods and process operating conditions. The method is based on thermodynamic principles and allows to determine the best heat exchangers network and utility system. It analyses possible heat exchanges between cold streams (requiring heat) and hot streams (releasing heat) in order to minimize irreversibilities. The process data is represented as a set of energy flows, or streams, as a function of heat load against temperature. These data are combined for all the streams in the plant to give composite curves, one for all "hot streams" (releasing heat) and one for all "cold streams" (requiring heat). The point of closest approach between the hot and cold composite curves is the pinch temperature (pinch point or just pinch), and is where design is most constrained. For both configurations, the minimum difference of temperature (ΔT_{min}) between hot fluids and cold fluids have been fixed to 10°C.

However, due to the complexity of the resulting heat exchangers network, a simplified network method has been used. This method will not lead to minimization of external heat requirement, but it will lead to the decreasing of the number of heat exchangers and the number of fluid splittings. This entails an advantage in perspective of a future economic analysis.

Anyhow, the difference in terms of energy efficiency are discussed in the following paragraph.

4.2.1. First configuration

At the outset, in order to reduce the number of streams involved in the thermal integration using the pinch analysis and the simplified network method, some flows have been integrated, checking that thermodynamic principles are not violated.

Moreover, since evaporating saturated water is used as cooling fluid in the "shell-and-tube" methanation reactors, the heat required for the evaporation of the saturated water is provided by the methanation reactions.

These integrations are shown in the following figure and are illustrated through red dashed lines.

Firstly, the pinch analysis methodology has been applied to the remaining stream, listed in Table 6.

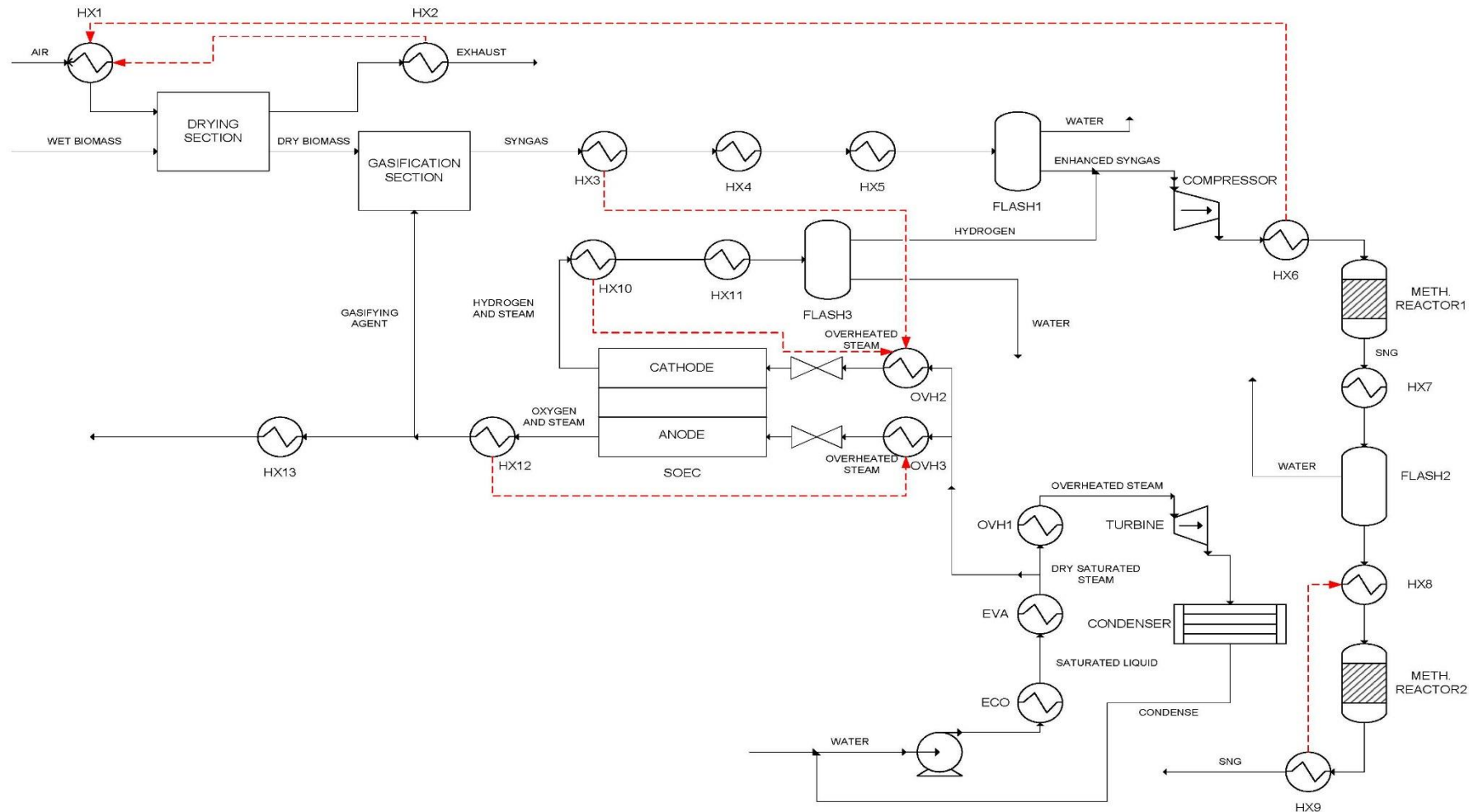


Figure 33 - Preliminary integration of some fluids in the first configuration

Stream	Type	T_{in} [°C]	T_{out} [°C]	Gc_p [kW/K]	Φ [kW]
Water	Cold	17,1	249,9	7,979	1857,97
Steam Rankine	Cold	249,9	524,8	1,617	444,34
Hot syngas	Hot	787,1	260	1,297	683,70
Syngas 1	Hot	260	66,6	1,197	231,50
Syngas 2	Hot	66,6	25	10,958	455,70
Hydrogen and steam 1	Hot	206,1	54,0	1,562	237,65
Hydrogen and steam 2	Hot	54,0	25	11,213	324,89
Oxygen and steam 1	Hot	100,1	81,3	1,057	19,90
Oxygen and steam 2	Hot	81,3	15	11,959	792,42
SNG 1	Hot	285	174,4	1,602	177,22
SNG 2	Hot	174,4	25	7,840	1170,99

Table 6 - List of streams involved in the thermal integration

The results of the pinch analysis methodology, in terms of temperature of pinch point, external heat requirement and waste heat, have been reported in Table 7. The pinch point represents the point in which minimum temperature of difference between hot and cold fluids occurs, the external heat requirement represents the difference between hot and cold fluids in the right side of the chart, the waste heat represents the difference between hot and cold composite curves in the left side of the chart.

Results	Value
Temperature of pinch point (T_{pp}^*) [°C]	169,4
External heat requirement [kW]	114,16
Waste heat [kW]	1905,82

Table 7 - Results of the pinch analysis applied to the first configuration

The composite curves, instead, are presented in Fig.34.

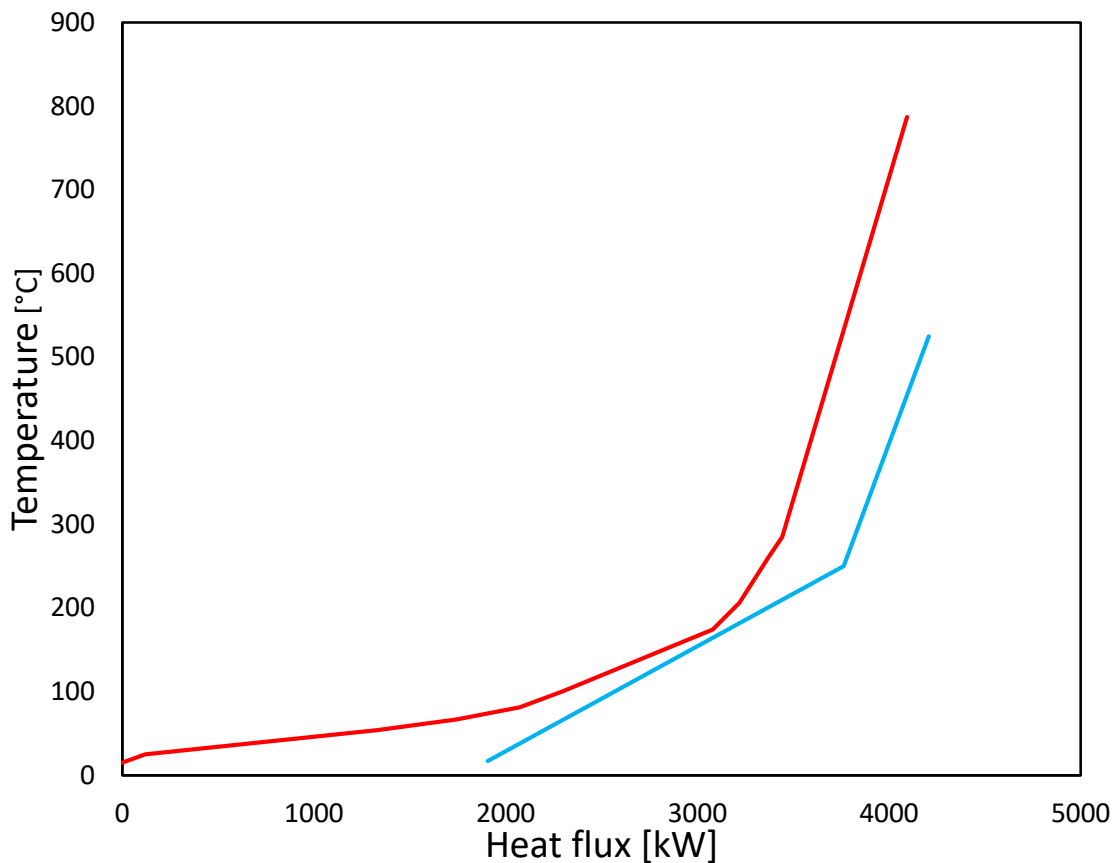


Figure 34 - Composite curves resulting from the pinch analysis applied to the first configuration

Finally, the results of the simplified network method have been reported in the following table.

Results	Value
External heat requirement [kW]	145,65
Waste heat [kW]	1967,14

Table 8 - Results of the simplified network method applied to the first configuration

4.2.2. Second configuration

Like in the first configuration, in order to reduce the number of streams involved in the thermal integration using the pinch analysis and the simplified network method, some flows have been integrated, checking that thermodynamic principles are not violated.

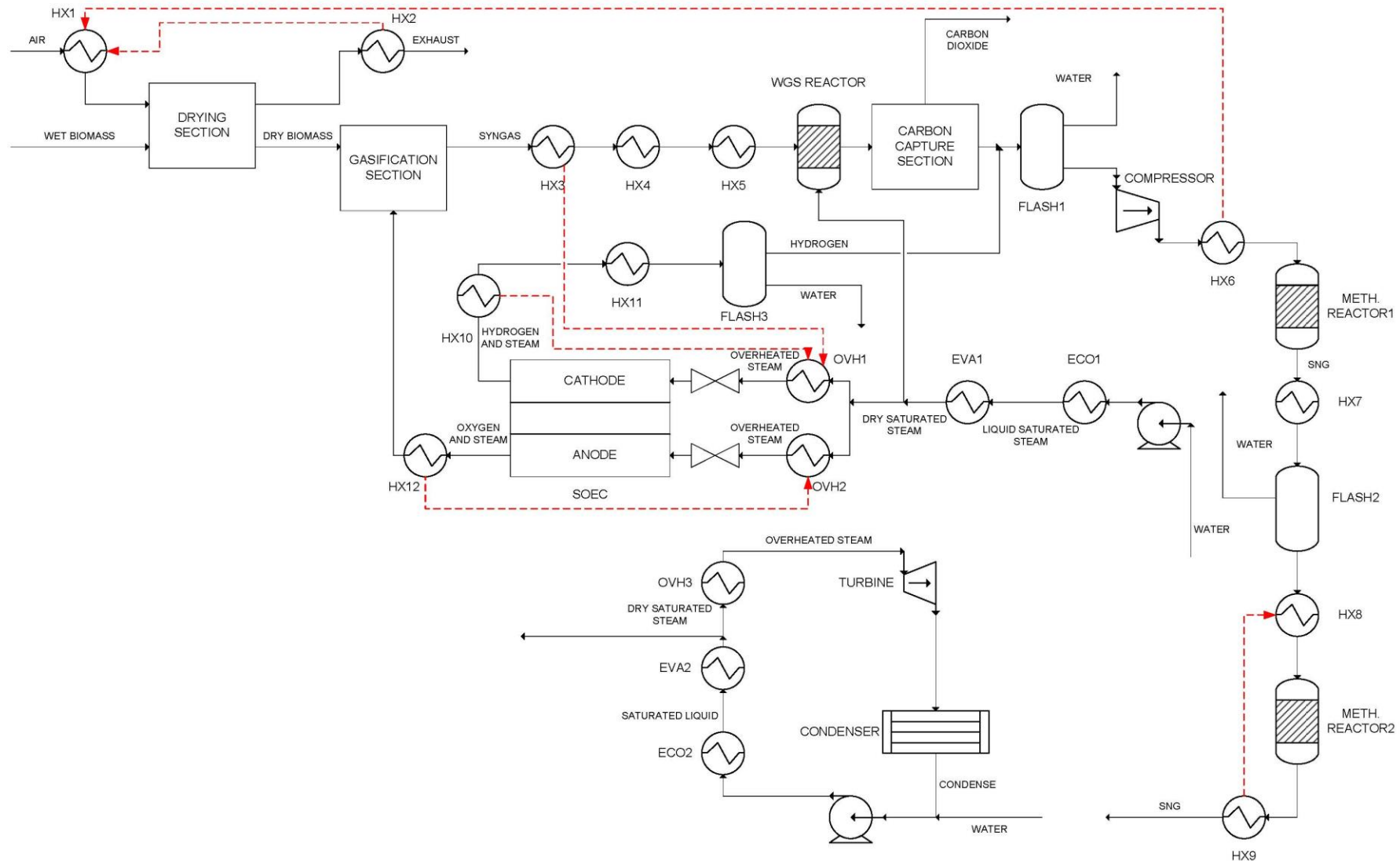
These integrations are shown in the following figure and are illustrated through red dashed lines.

However, differently from the first configuration, the heat required for the carbon capture section must be taken into account. Ferrara et al. [18] described a post combustion carbon capture plant based on chemical absorption using monoethanolamine sorbent. For what concerns the thermal integration, the only component that requires external heat is the reboiler. The reboiler duty indicated from the authors is 4300 kJ/kg. Therefore, a heat balance has been performed in order to check if the excess heat, in terms of dry saturated steam produced in the methanation reactors, is sufficient to satisfy the heat requirement of the reboiler. Moreover, also the heat provided by the water gas shift reactor contributes to satisfy this requirement.

Quantity	Value
Reboiler duty [kJ/kg]	4300
Mass flow rate of CO ₂ captured [kg/s]	0,368
Heat provided by methanation reactors [kW]	1663,46
Heat provided by water gas shift reactor [kW]	536,43
Heat required for the evaporators inside the plant [kW]	-743,65
Heat required for carbon capture [kW]	-1582,31
Heat balance	-126,07

Table 9 - Heat balance for the second configuration

So, an extra amount of heat, in terms of dry saturated steam, must be supplied to the reboiler of the carbon capture section. This quantity is provided by the cooling of the syngas, subtracting, nevertheless, a significant portion of heat from the Rankine cycle.



The pinch analysis methodology has been applied to the remaining stream, listed in Table 10.

Stream	Type	T_{in} [°C]	T_{out} [°C]	Gc_p [kW/K]	Φ [kW]
Water	Cold	17,1	249,9	2,363	550,27
Water Rankine	Cold	17,1	675,5	0,912	600,63
Syngas 1	Hot	772,1	250	1,292	674,86
Syngas 2	Hot	197,5	30	1,491	249,77
Hydrogen and steam 1	Hot	206	54,0	0,385	58,56
Hydrogen and steam 2	Hot	54,0	15	2,361	92,02
SNG 1	Hot	285	181,9	1,069	110,21
SNG 2	Hot	181,9	25	5,968	936,35

Table 10 - List of streams involved in the thermal integration

The results of the pinch analysis methodology, in terms of temperature of pinch point, external heat requirement and waste heat, have been reported in Table 7. The pinch point represents the point in which minimum temperature of difference between hot and cold fluids occurs, the external heat requirement represents the difference between hot and cold fluids in the right side of the chart, the waste heat represents the difference between hot and cold composite curves in the left side of the chart.

Results	Value
Temperature of pinch point (T_{pp}^*) [°C]	176,9
External heat requirement [kW]	0
Waste heat [kW]	970,88

Table 11 - Results of the pinch analysis applied to the second configuration

The composite curves, instead, are presented in Figure 35.

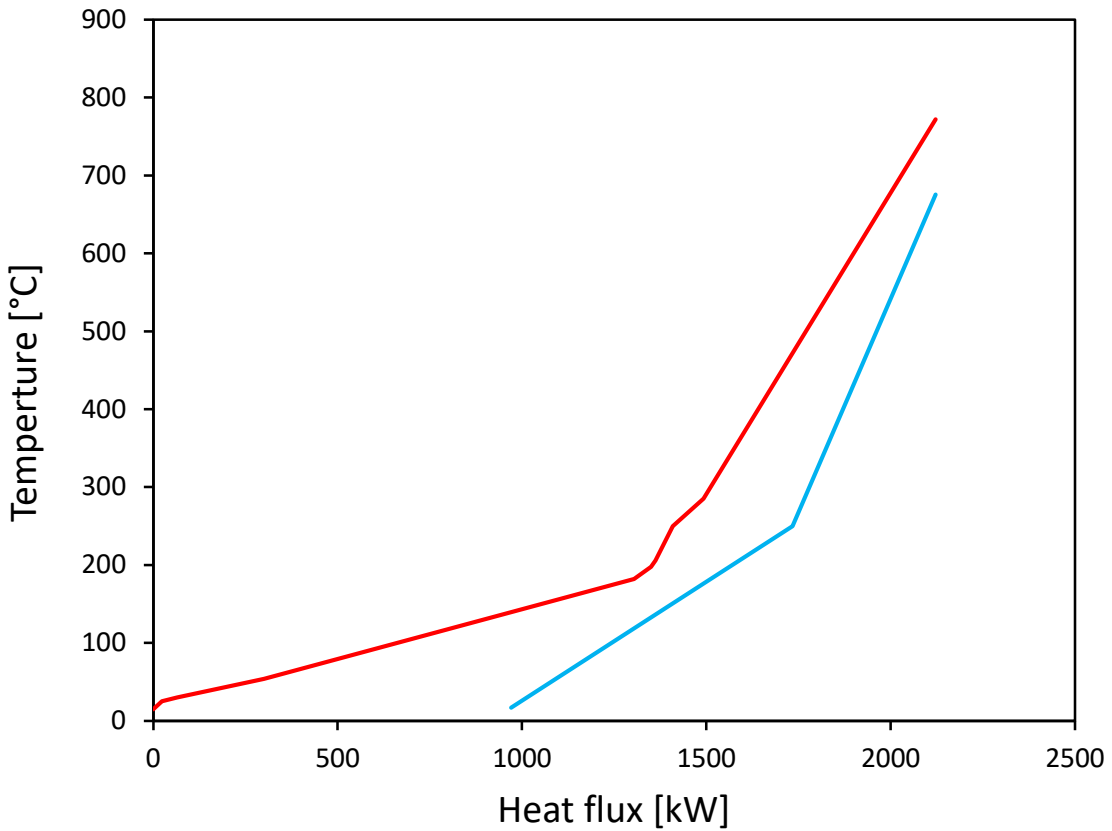


Figure 35 - Composite curves resulting from the pinch analysis applied to the second configuration

Finally, the results of the simplified network method have been reported in the following table.

Results	Value
External heat requirement [kW]	75,99
Waste heat [kW]	983,87

Table 12 - Results of the simplified network method applied to the second configuration

4.3. Energy efficiency

Finally, the energy efficiency has been computed for both the configurations. It has been computed as the ratio between the chemical power of the synthetic natural gas produced and the sum of the chemical power of the biomass considered and all the other power input. The power produced by the Rankine cycle is subtracted to the denominator, since it has been supposed that it is used to reduce the energy requirement of the plant. Table 13 and 14 report all the data needed for the calculation of the energy efficiency.

	Value
Lower Heating Value of the beech [MJ/kg]	14,71
Beech mass flow rate [kg/s]	0,5
Electric power required by the SOEC [MW]	11,23
Electric power required by the compressor [MW]	1,05
Electric power required by the heaters [MW]	0,15
Electric power required by the pump [MW]	0,026
Lower Heating Value of the SNG produced [MJ/kg]	48,11
SNG mass flow rate [kg/s]	0,285
Mechanical power produced by the turbine [MW]	0,735
Energy efficiency	0,731

Table 13 - Parameters for the calculation of the energy efficiency of the first layout

The lower heating value of the biomass utilized is taken from Phyllis2 database [16]. All the other data represent the results of the Aspen Plus™ simulation. Since the electric power required by the SOEC must be in direct current, an AC-DC converter (rectifier) is needed in order to convert the electrical power withdrawn from the grid in alternate current to power in direct current. An efficiency of 0,98 has been considered for the rectifier.

	Value
Lower Heating Value of the beech [MJ/kg]	14,71
Beech mass flow rate [kg/s]	0,5
Electric power required by the SOEC [MW]	2,71
Electric power required by the compressor [MW]	0,624
Electric power required by the heaters [MW]	0,076
Electric power required by the pump [MW]	0,007
Lower Heating Value of the SNG produced [MJ/kg]	48,47
SNG mass flow rate [kg/s]	0,150
Mechanical power produced by the turbine [MW]	0,214
Energy efficiency	0,685

Table 14 - Parameters for the calculation of the energy efficiency of the second layout

As expected, the first layout of the plant presents a higher energy efficiency, since all the dry saturated steam in excess is destined to the Rankine cycle. Instead in the second layout of the plant, the dry saturated steam in excess and part of the heat due to the cooling of the syngas is destined to the carbon capture section.

Finally, the following table shows the difference in energy efficiency in the case of thermal integration performed with pinch analysis and in the case of thermal integration performed with the simplified network method.

Configuration	Energy efficiency with thermal integration based on pinch analysis	Energy efficiency with thermal integration based on simplified network method
First	0,733	0,731
Second	0,689	0,685

Table 15 - Comparison of energy efficiency with the different thermal integration method

Obviously, carrying out the thermal integration with pinch analysis method, a higher value of the energy efficiency has been obtained. However, because of the complexity of the resulting heat exchangers network, the simplified network method could be

preferable, since it leads to a simpler heat exchangers network and this is a positive factor in view of an economic analysis. Anyhow, the benefits in terms of efficiency obtained with the thermal integration carried out with pinch analysis method should be compared with the benefits in terms of economic savings obtained with the thermal integration carried out with the simplified network method.

5. Conclusions

A plant combining a gasifier, a solid oxide-based electrolyser cell and a methanator has been designed and studied.

Two configurations of this plant have been proposed: the first one is simpler but requires a SOEC of a larger size in order to hydrogenate the syngas produced by the gasifier, while the second one is more complex since the SOEC does not provide the amount of hydrogen that satisfy the requirement of the subsequent methanation section and then a water gas shift reactor and a carbon capture and sequestration section are needed.

The two configurations have been compared at the same conditions of gasification. For this reason, a preliminary gasification study was carried out, in order to find the optimal gasification conditions for the proposed plant.

The thermal integration of the streams of the plant using pinch analysis methodology and using a simplified network method that is able to reduce the complexity of the heat exchangers network has been performed.

Finally, the energy efficiency of both configurations has been calculated. As expected, the energy efficiency of the first configuration results to be higher than the energy efficiency of the second one.

Future developments of this work could include:

- the economic analysis of both configurations, so as to evaluate the capital costs, to assess the as-produced SNG cost allowing for economic feasibility of the initial capital investments and to compare this cost with current average price of natural gas;
- the production of other types of biofuels, such as methanol, dimethyl ether or Fischer-Tropsch fuels;
- the intermittent operation of the electrolyser only, with gas storage available for the products of the SOEC to allow a continuous operation of the gasifier and the methane synthesis reactor;
- the use of a kinetic approach for all the reactors of the plant, so as to meet results closer to reality

Bibliography

- [1] International Energy Agency, "Statistics | World - Total Primary Energy Supply (TPES) by source (chart)." 2012.
- [2] International Energy Agency, "CO₂ Emissions.". Available: <https://www.iea.org/statistics/co2emissions/>.
- [3] M. Pozzo, A. Lanzini, and M. Santarelli, "Enhanced biomass-to-liquid (BTL) conversion process through high temperature co-electrolysis in a solid oxide electrolysis cell (SOEC)," *Fuel*, vol. 145, pp. 39–49, 2015.
- [4] L. R. Clausen, N. Houbak, and B. Elmegaard, "Technoeconomic analysis of a methanol plant based on gasification of biomass and electrolysis of water," *Energy*, vol. 35, no. 5, pp. 2338–2347, 2010.
- [5] Q. Bernical, X. Joulia, I. Noirot-Le Borgne, P. Floquet, P. Baurens, and G. Boissonnet, "Sustainability assessment of an integrated high temperature steam electrolysis-enhanced biomass to liquid fuel process," *Ind. Eng. Chem. Res.*, vol. 52, no. 22, pp. 7189–7195, 2013.
- [6] L. R. Clausen, "Energy efficient thermochemical conversion of very wet biomass to biofuels by integration of steam drying, steam electrolysis and gasification," *Energy*, vol. 125, pp. 327–336, 2017.
- [7] A. Gambhir, S. Few, J. Nelson, A. Hawkes, O. Schmidt, and I. Staffell, "Future cost and performance of water electrolysis: An expert elicitation study," *Int. J. Hydrogen Energy*, vol. 42, no. 52, pp. 30470–30492, 2017.
- [8] A. Molino, S. Chianese, and D. Musmarra, "Biomass gasification technology: The state of the art overview," *J. Energy Chem.*, vol. 25, no. 1, pp. 10–25, 2016.
- [9] S. K. Sansaniwal, K. Pal, M. A. Rosen, and S. K. Tyagi, "Recent advances in the development of biomass gasification technology: A comprehensive review," *Renew. Sustain. Energy Rev.*, vol. 72, no. December 2015, pp. 363–384, 2017.
- [10] N. Abdoulmoumine, S. Adhikari, A. Kulkarni, and S. Chattanathan, "A review on biomass gasification syngas cleanup," *Appl. Energy*, vol. 155, pp. 294–307, 2015.
- [11] E. Giglio, A. Lanzini, M. Santarelli, and P. Leone, "Synthetic natural gas via integrated high-temperature electrolysis and methanation: Part I-Energy performance," *J. Energy Storage*, vol. 1, no. 1, pp. 22–37, 2015.
- [12] L. Barelli, G. Bidini, and G. Cinti, "Steam as sweep gas in SOE oxygen electrode," *J. Energy Storage*, vol. 20, no. September, pp. 190–195, 2018.
- [13] M. Zaman and J. H. Lee, "Carbon capture from stationary power generation sources: A review of the current status of the technologies," *Korean J. Chem. Eng.*, vol. 30, no. 8, pp. 1497–1526, 2013.
- [14] U. Henriksen, J. Ahrenfeldt, T. Kvist, and B. Gøbel, "The design , construction and operation of a 75 kW two-stage gasifier," vol. 31, pp. 1542–1553, 2006.

- [15] M. La Villetta, M. Costa, and N. Massarotti, “Modelling approaches to biomass gasification: A review with emphasis on the stoichiometric method,” *Renew. Sustain. Energy Rev.*, vol. 74, no. February, pp. 71–88, 2017.
- [16] “Phyllis2 - Database for biomass and waste.” [Online]. Available: <https://phyllis.nl/>.
- [17] E. Giglio *et al.*, “Power-to-Gas through High Temperature Electrolysis and Carbon Dioxide Methanation: Reactor Design and Process Modeling,” *Ind. Eng. Chem. Res.*, vol. 57, no. 11, pp. 4007–4018, 2018.
- [18] G. Ferrara, A. Lanzini, P. Leone, M. T. Ho, and D. E. Wiley, “Exergetic and exergoeconomic analysis of post-combustion CO₂ capture using MEA-solvent chemical absorption,” *Energy*, vol. 130, pp. 113–128, 2017.